NEDC-23677
CLASS II
SEPTEMBER 1977

EMPLOYEES ONLY

DUANE ARNOLD FEEDWATER NOZZLE TEMPERATURE CYCLING

J. E. CHARNLEY

GENERAL ELECTRIC

NEDC-23677
Class II
September 1977

EMPLOYEES ONLY

DUANE ARNOLD FEEDWATER NOZZLE TEMPERATURE CYCLING

J. E. Charnley

Approved:
N. J. Biglieri, Manager
Reactor Assembly and Pressure
Vessel Design

BOILING WATER REACTOR PROJECTS DEPARTMENT • GENERAL ELECTRIC COMPANY
SAN JOSE, CALIFORNIA 95125
GENERAL ELECTRIC

DISCLAIMER OF RESPONSIBILITY

This document was prepared by or for the General Electric Company. Neither the General Electric Company nor any of the contributors to this document:

A. *Makes any warranty or representation, express or implied, with respect to the accuracy, completeness, or usefulness of the information contained in this document, or that the use of any information disclosed in this document may not infringe privately owned rights; or*

B. *Assumes any responsibility for liability or damage of any kind which may result from the use of any information disclosed in this document.*

TABLE OF CONTENTS

		Page
	ABSTRACT	ix
1.0	INTRODUCTION	1-1
2.0	SUMMARY AND CONCLUSIONS	2-1
3.0	DISCUSSION	3-1
	3.1 Feedwater Sparger and Nozzle Design	3-1
	3.2 Instrumentation Installation	3-1
	3.3 Monitoring	3-4
	3.4 Data	3-5
	3.5 Criteria	3-28
	3.6 Analysis	3-31
4.0	REFERENCES	4-1
	DISTRIBUTION	1

LIST OF ILLUSTRATIONS

Figure	Title	Page
3-1	Original Geometry	3-2
3-2	Sensor Locations	3-3
3-3	Temperature Cycling Turbine Trip Recorder 1	3-6
3-4	Temperature Cycling Turbine Trip Recorder 2	3-7
3-5	Temperature Cycling Turbine Trip Recorder 3	3-8
3-6	Temperature Cycling 22.4% Power Recorder 1	3-9
3-7	Temperature Cycling 22.4% Power Recorder 2	3-10
3-8	Temperature Cycling 22.4% Power Recorder 3	3-11
3-9	Temperature Cycling 50.2% Power Recorder 1	3-12
3-10	Temperature Cycling 50.2% Power Recorder 2	3-13
3-11	Temperature Cycling 50.2% Power Recorder 3	3-14
3-12	Temperature Cycling 73.6% Power Recorder 1	3-15
3-13	Temperature Cycling 73.6% Power Recorder 2	3-16
3-14	Temperature Cycling 73.6% Power Recorder 3	3-17
3-15	Temperature Cycling 84.5% Power Recorder 1	3-18
3-16	Temperature Cycling 84.5% Power Recorder 2	3-19
3-17	Temperature Cycling 84.5% Power Recorder 3	3-20
3-18	Temperature Cycling N4A(45°) Nozzle	3-21
3-19	Temperature Cycling N4B (135°) Nozzle	3-22
3-20	Temperature Cycling N4C (225°) Nozzle	3-23
3-21	Temperature Cycling N4D (315°) Nozzle	3-24
3-22	Temperature Cycling Bounding Curve	3-25
3-23	Illustration of Ordered Overall Range (OOR) Cycle Counting Approach	3-33
3-24	Load Spectra	3-36
3-25	GE Extrapolation of ASME Fatigue Curve	3-38
3-26	Fatigue Damage Curve	3-39

LIST OF TABLES

Table	Title	Page
3-1	Maximum Peak-to-Peak Temperature Range in Approximately 4-Minute Interval	3-26
3-2	May 1977 Startup Map	3-29
3-3	40-Year Design Life Time/Temperature	3-30
3-4	Envelope Spectrum for Fatigue Damage Calculation	3-35
3-5	Cumulative Fatigue Damage	3-40

ABSTRACT

All four Iowa Electric Duane Arnold Nuclear Reactor feedwater nozzles were instrumented with resistance temperature detectors during the May 1977 outage and the subsequent startup was monitored. The measured thermal cycling was significantly less than at reactors which have had significant cracking. Recommendations for future inspections are presented based on resultant fatigue damage calculations.

ACKNOWLEDGEMENTS

The author acknowledges the contributions made to this report by the following individuals:

G. G. Chen
S. A. Delvin
A. B. Fife
J. N. Loofbourrow
K. R. Miller
P. C. Riccardella
C. R. Toye

1.0 INTRODUCTION

The inner blend radius of the four Duane Arnold Nuclear Reactor feedwater nozzles were instrumented with resistance temperature detectors during the scheduled refueling outage which began in April 1977. The purpose of the instrumentation was to record the temperature cycling experienced by each feedwater nozzle due to the mixing of feedwater and reactor downcomer water. This cycling has caused feedwater nozzle cracking at other BWRs.

The Duane Arnold feedwater nozzle/thermal sleeve/sparger design is unique. It was postulated that the potential for nozzle cracking at Duane Arnold was less than at other reactors which have experienced cracking.

This report describes the instrumentation installation, summarizes the data, gives the criteria for evaluating the data, describes the method of analysis and presents recommendations for further inspections.

2.0 SUMMARY AND CONCLUSIONS

The Duane Arnold feedwater nozzle design was specifically exempted from the General Electric Feedwater Nozzle Interim Examination Recommendation (FNIER) contained in Service Information Letter (SIL) Number 207, because the feedwater nozzle thermal sleeve is welded to the nozzle safe end. Therefore, it was expected that the feedwater nozzles would experience less thermal cycling and thus significantly less cracking than other BWRs with a similar period of operation.

The feedwater nozzle temperature cycling recorded during the May 1977 startup was significantly less than that recorded for other BWRs which have a slip fit between the thermal sleeve and the safe end. Large thermal cycles do not occur at Duane Arnold at low feedwater temperatures. The peak-to-peak temperature cycling is between 59°F and 82°F for all conditions with the feedwater temperature greater than 200°F. At lower feedwater temperatures the cycling is reduced except during a turbine trip transient.

Iowa Electric supplied the basis for a time/temperature map for the feedwater system at Duane Arnold. Based on the time/temperature map and on the measured temperature cycling, a 40-year cumulative fatigue usage factor due to rapid thermal cycling of 0.20 was calculated. This value is low enough so that feedwater nozzle cracking due to fatigue is not predicted to occur. Should cracking due to another mechanism occur, then the cracks will propagate slower than at other BWRs because of the smaller thermal cycles experienced at Duane Arnold.

It is therefore recommended that Duane Arnold remain exempt from FNIER. Periodic ultrasonic examination of the feedwater nozzles is recommended to assure that significant cracking due to another mechanism has not occurred. Liquid penetrant examination of the feedwater nozzle and safe end is not required, unless the ultrasonic examination detects cracking. To assess the performance of the thermal sleeve with time, it is also recommended that periodic visual examination of the feedwater sparger and of the weld between the thermal sleeve and safe end be performed.

3.0 DISCUSSION

3.1 FEEDWATER SPARGER AND NOZZLE DESIGN

The original Duane Arnold feedwater nozzle/thermal sleeve/sparger design is unique. The thermal sleeve was field welded to the nozzle safe end. The sparger was assembled to the thermal sleeve with a maximum diametral clearance of 0.004 inch. Thus leakage cannot occur between the thermal sleeve and the nozzle as it can with the original slip fit design at other BWRs. However, leakage can occur between the sparger tee box and the thermal sleeve. Figure 3-1 shows the original design. The original design details are given in References 1 through 4.

BWR SIL Number 207 "Feedwater Nozzle Interim Examination Recommendation" does not apply to Duane Arnold due to the thermal sleeve to nozzle weld. Thus, the type and frequency of feedwater nozzle examinations must be evaluated specifically for Duane Arnold. To help establish a basis for this evaluation the feedwater nozzles were instrumented during the April 1977 refueling outage.

3.2 INSTRUMENTATION INSTALLATION

Ailtech SG725 Resistance Temperature Detector (RTD) (similar to those used at other reactors) were installed on all four feedwater nozzles. The RTD platinum-tungsten element is spiral wound and enclosed in a stainless steel housing, which is filled with MgO insulation. The housing is flanged to facilitate a spot welding application. The sensor is hermetically sealed, and includes an integral stainless steel cable. Each RTD was configured into a single active arm, three lead wire, Wheatstone bridge system, and calibrated at 212 and 550°F. An RTD requires less than 0.4 sec to achieve 90% of its final value following a step change in temperature from 32°F to 550°F.

The RTD locations are shown on Figure 3-2. The locations were selected based on the following criteria:

a. General Electric testing of tee-box sparger designs indicated that maximum cycling on the Duane Arnold feedwater nozzles would occur on the bottom ($\theta = 180^{\circ}$) of the nozzle and would occur on the

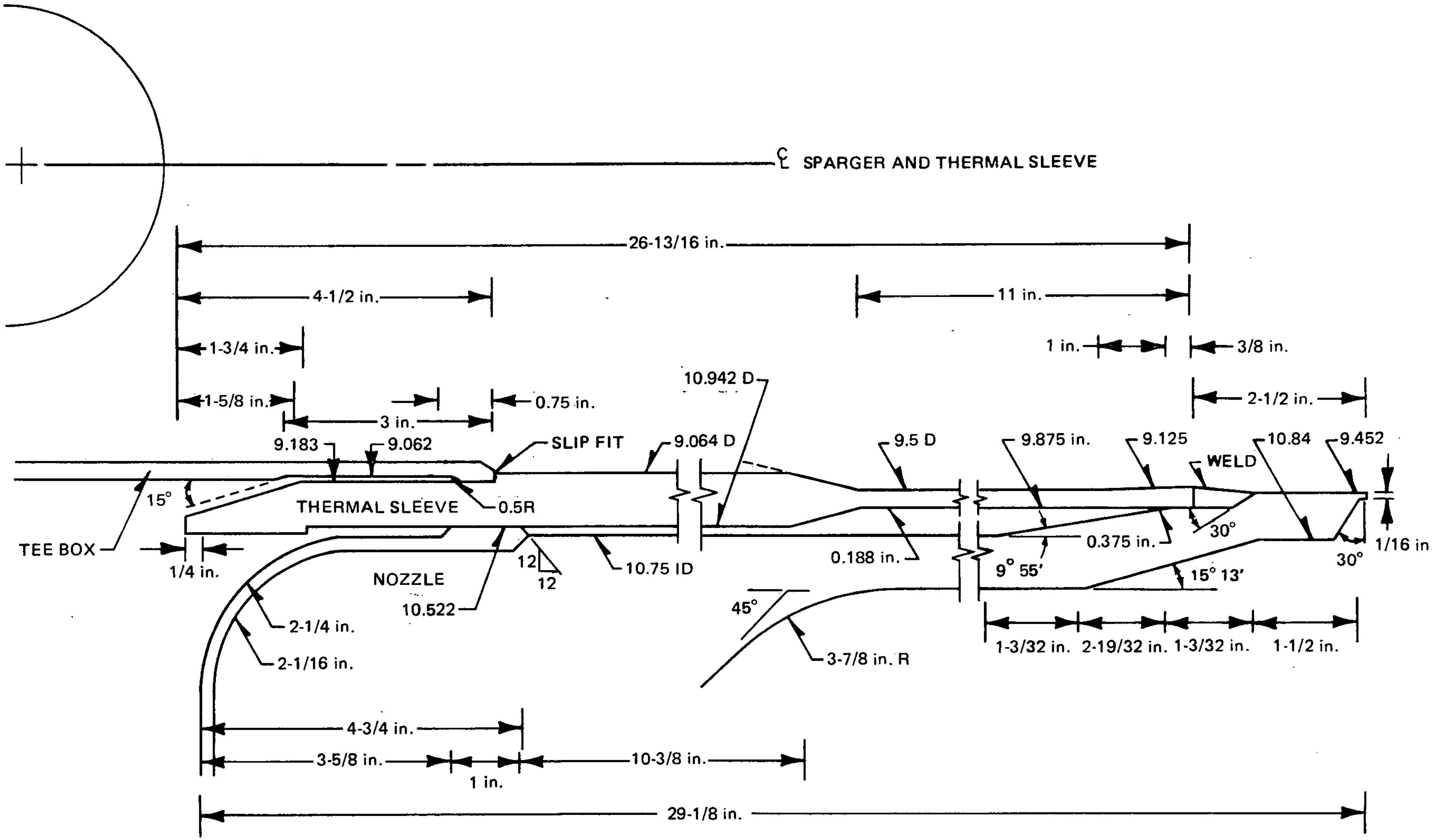

Figure 3-1. Original Geometry

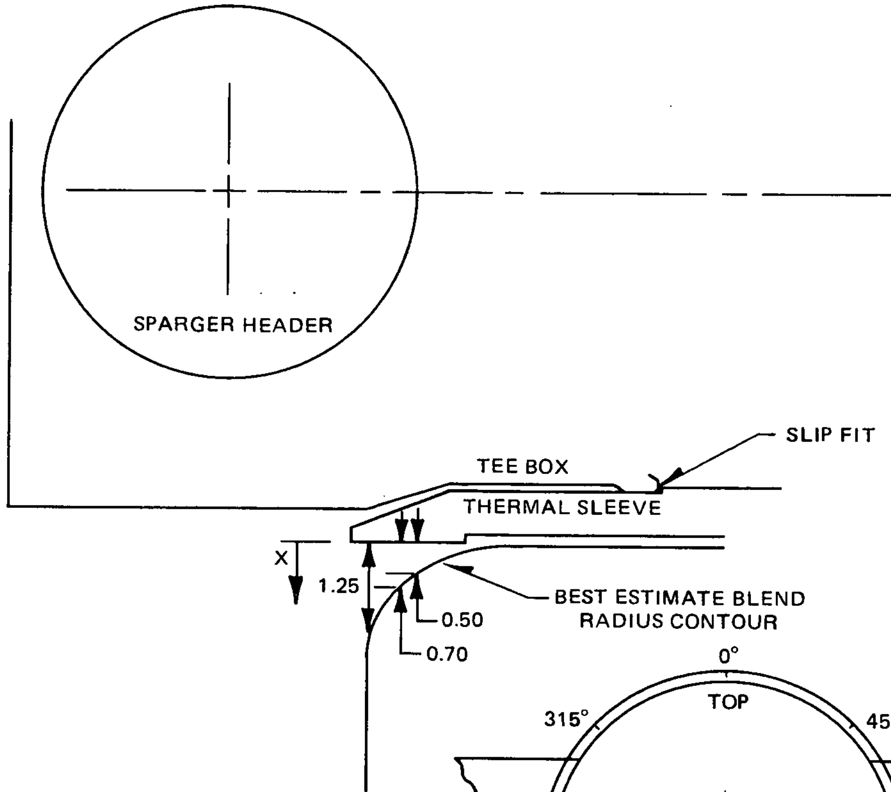

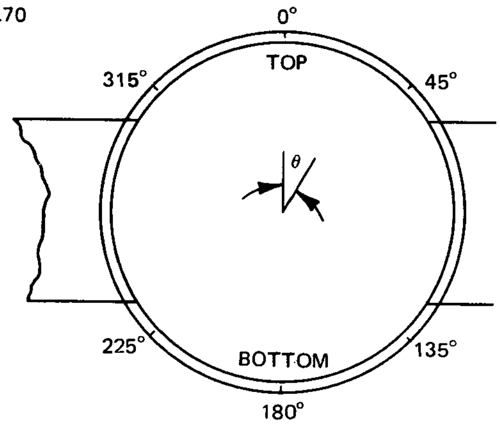

SPARE SENSOR LOCATIONS

SENSOR	NOZZLE	X	θ	ADJACENT PRIME SENSOR
SNA	45°	1.45	180°	T11
SNB	135°	0.7	180°	T13
SNC	225°	0.7	180°	T4
SND	315°	0.7	180°	T9

PRIME SENSOR LOCATIONS

	NOZZLE	SENSOR 1 X	SENSOR 1 θ	SENSOR 2 X	SENSOR 2 θ	SENSOR 3 X	SENSOR 3 θ	SENSOR 4 X	SENSOR 4 θ	SENSOR 5 X	SENSOR 5 θ	SENSOR 6 X	SENSOR 6 θ
		(T1)		(T2)		(T3)		(T4)		(T5)		(T6	
N4C	225°	0.50	0°	0.50	45°	0.50	135°	0.50	180°	0.50	225°	0.50	315°
		(T7)		(T8)		(T9)							
N4D	315°	0.50	0°	1.25	0°	0.50	180°						
		(T10)		(T11)									
N4A	45°	0.50	180°	1.25	180°								
		(T13)		(T12)		(T14)							
N4B	135°	0.50	180°	0.50	135°	0.50	225°						

RECORDER	LOCATION 1	LOCATION 2	LOCATION 3	LOCATION 4	LOCATION 5	LOCATION 6
1	(T1) N4C1	(T2) N4C2	(T3) N4C3	(T4) N4C4	(T5) N4C5	(T6) N4C6
2	(T4) N4C4	(T9) N4D3	(T10) N4A1	(T13) N4B1	(T12) N4B2	(T14) N4B3
3	(T7) N4D1	(T8) N4D2	(T9) N4D3	(T10) N4A1	(T11) N4A2	

Figure 3-2. Sensor Locations

nozzle blend radius ($X \simeq 0.5$). Temperature cycling on the nozzle bore and on the safe end should be significantly less than on the blend radius.

b. One location ($\theta = 180^\circ$ and $X = 0.50$) was instrumented on all four nozzles.

c. The N4C nozzle has six RTDs to determine magnitude of cycling as a function of azimuthal position.

d. The N4A and N4D nozzles have three and four RTDs, respectively, to determine magnitude of cycling as a function of location on blend radius (dimension X).

e. The N4B nozzle has three RTDs to confirm azimuthal dependence as measured on the N4C nozzle.

f. To allow adequate room for installation, the minimum distance between a sensor and the thermal sleeve was 0.5 inch.

All 18 RTDs (14 prime labeled T1 through T14 and 4 spare labeled SNA through SND) were installed without loss. All 18 sensors remained operational during the entire test. The installation details are given in References 5 through 8.

3.3 MONITORING

The RTDs were attached to strip chart recorders. Figure 3-2 shows how the sensors are wired to the chart recorders. Recorder Number 1 has the six N4C RTDs. Thus, it shows the azimuthal variation of cycling. Recorder Number 2 has the common RTD ($X = 0.5$, $\theta = 180^\circ$) location, as well as the RTDs along the bottom half of the N4B nozzle. Thus, it will show the nozzle to nozzle variation of thermal cycling and the N4B azimuthal cycling variation. Recorder Number 3 has the N4A and N4D RTDs. Thus, it will show the cycling magnitude as a function of position along the blend radius. The spare sensors were periodically monitored by replacing prime sensors from a recorder.

The entire startup from May 12, 1977 to May 20, 1977 was monitored. The majority of time the recorders were set on slow speed (0.5 mm/sec). At selected times the chart speed was increased to 10 mm/sec.

3.4 DATA

3.4.1 Temperature Fluctuations

The entire startup from 2000 hours on May 12,1977 to 1400 hours on May 20 was recorded. The startup lasted 187 hours and 167 hours of data were obtained. The missing 20 hours were distributed throughout the startup, and were caused by various equipment malfunctions. During the initial startup phase the only significant temperature cycling occurred during the turbine trip. The turbine trip cycling is shown on Figures 3-3 through 3-5. The highest cycling was recorded by sensors T4, T9, T10, and T13, which are at the bottom ($X = 0.50$, $\theta = 180^\circ$) of nozzles N4C, N4D, N4A, and N4B, respectively. The maximum cycling is 115°F peak-to-peak. As can be seen in the figures, the number of significant thermal cycles is small and the time during which the cycling occurs is short (less than 1 hour).

Figures 3-6 through 3-17 show approximately 1 minute of temperature cycling for four power levels 22.4%, 50.2%, 73.6% and 84.5%, which was the highest power level achieved during the test. The maximum and minimum peak-to-peak cycling for each temperature sensor for each power level for a 4 minute interval are tabulated on Table 3-1 and plotted in Figures 3-18 through 3-21.

Figure 3-22 is a bounding curve of the maximum peak-to-peak cycling using all the RTDs.

Inspection of Figures 3-18 through 3-22 and Table 3-1 will reveal that:

a. The highest cycling occurs on nozzle N4A (45°).

b. The maximum cycling occurs at or near the bottom of all nozzles.

c. The highest cycling value exclusive of the turbine trip transient was 82°F and was recorded by T11 at 22.4% power. Inspection of the

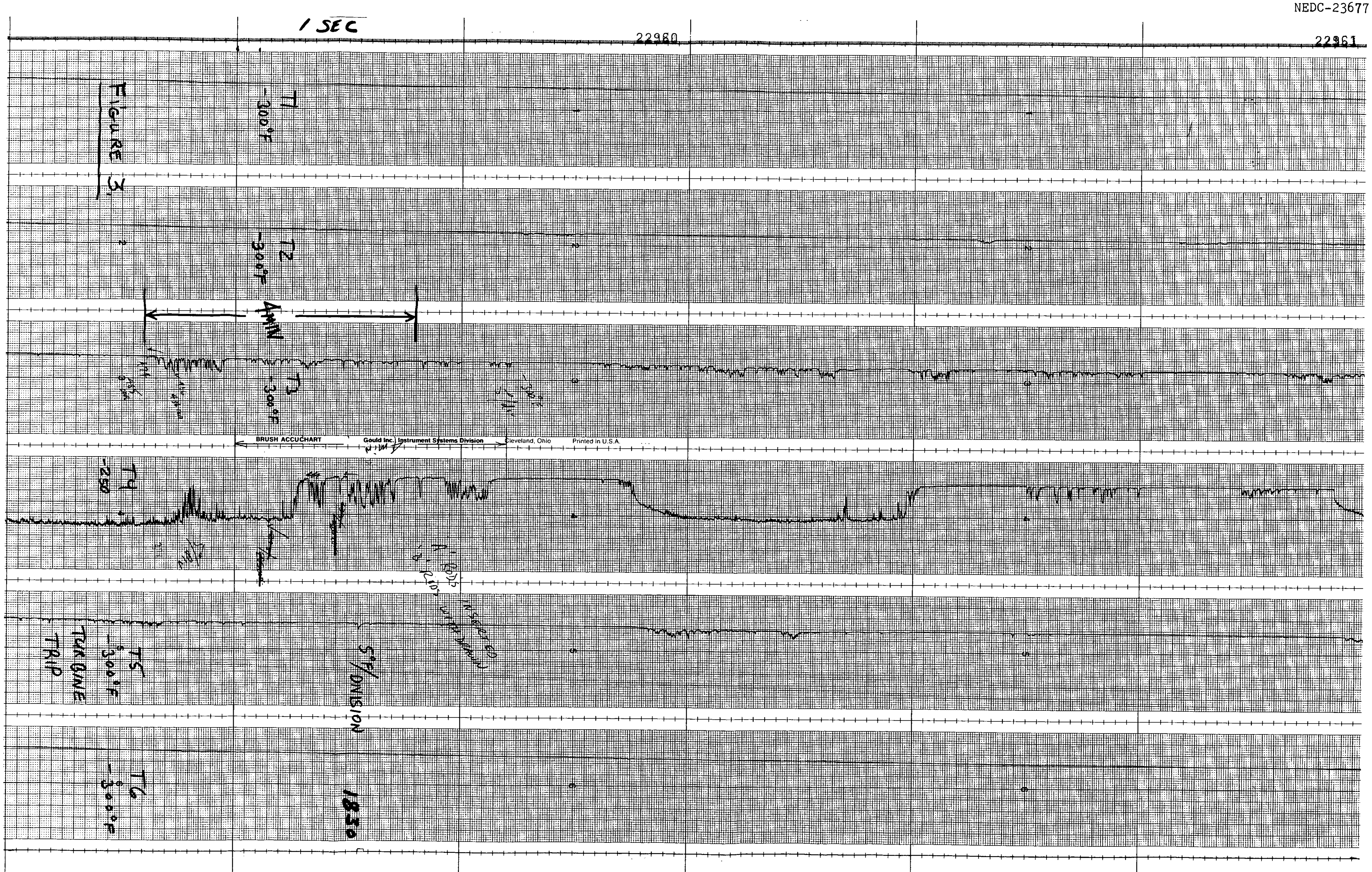

Figure 3-3. Temperature Cycling Turbine Trip Recorder 1

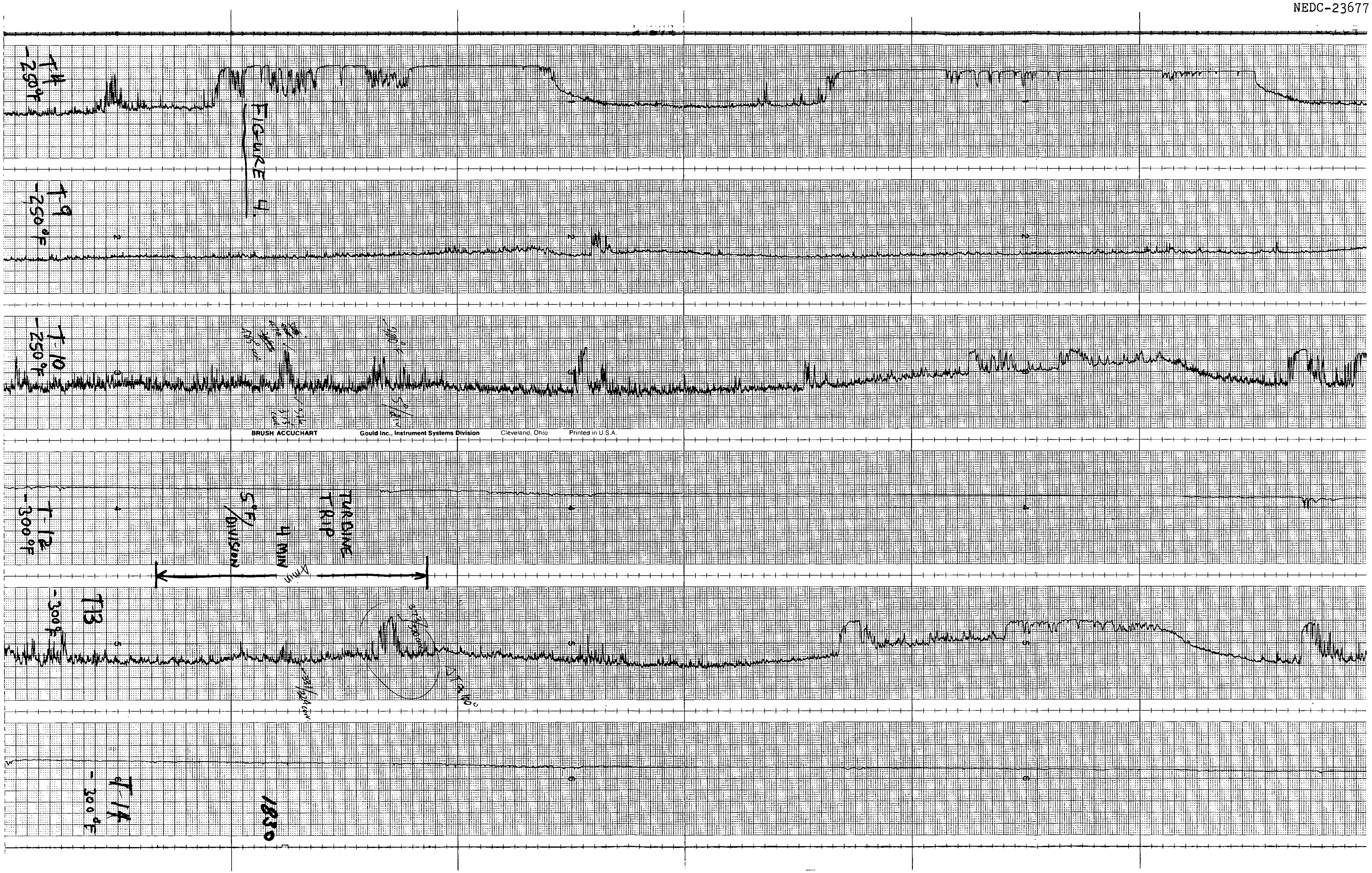

Figure 3-4. Temperature Cycling Turbine Trip Recorder 2

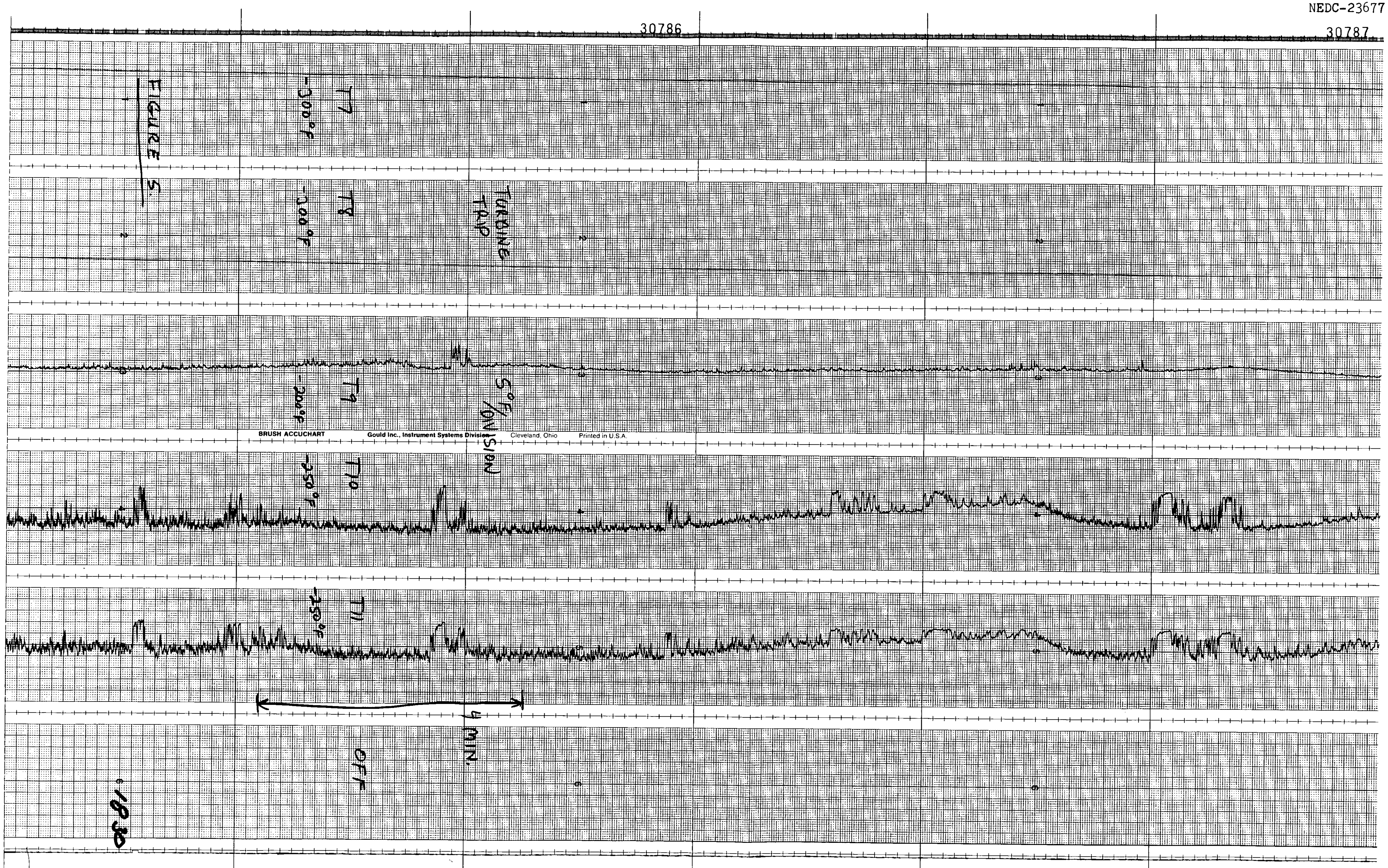

Figure 3-5. Temperature Cycling Turbine Trip Recorder 3

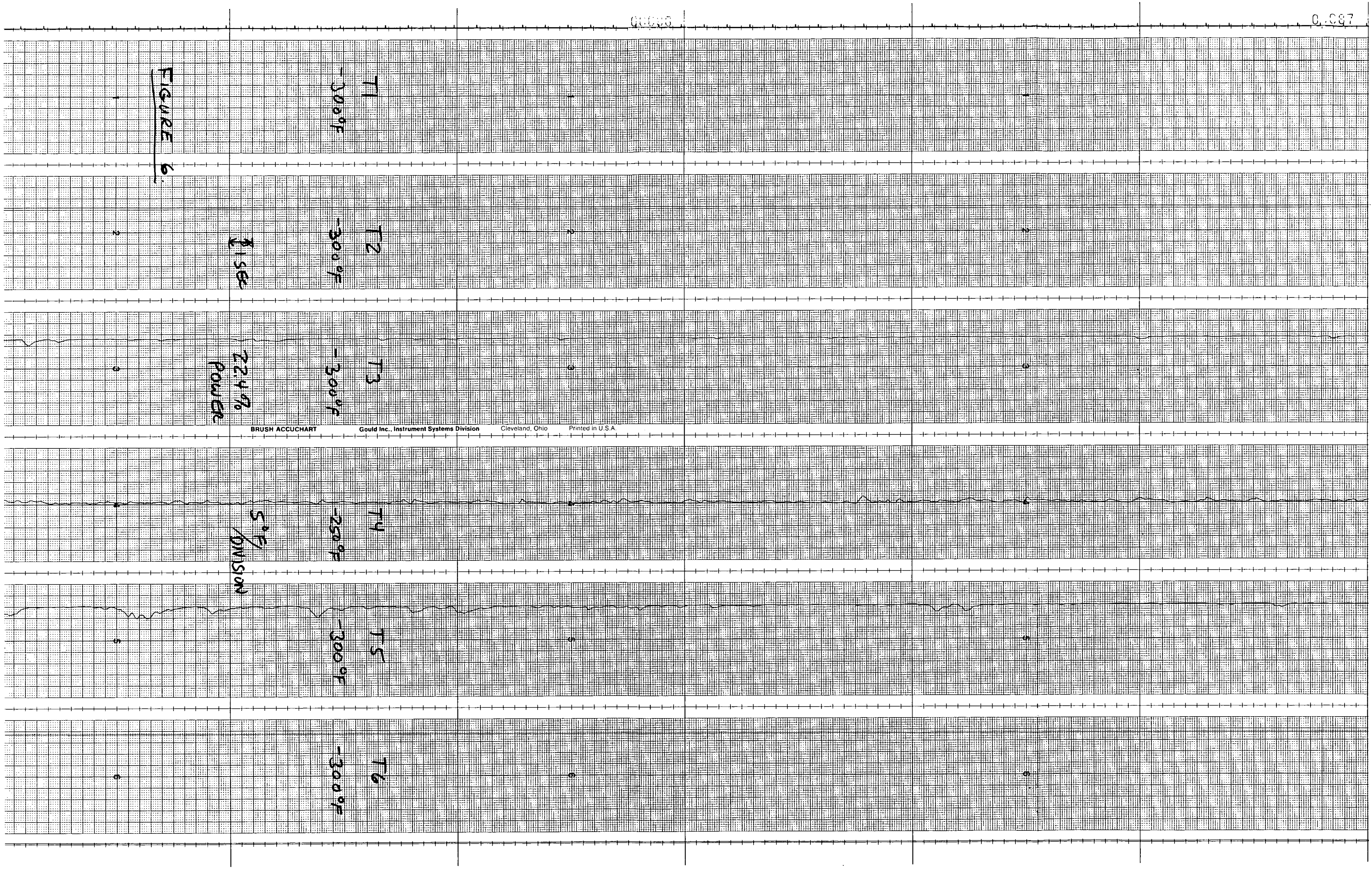

Figure 3-6. Temperature Cycling 22.4% Power Recorder 1

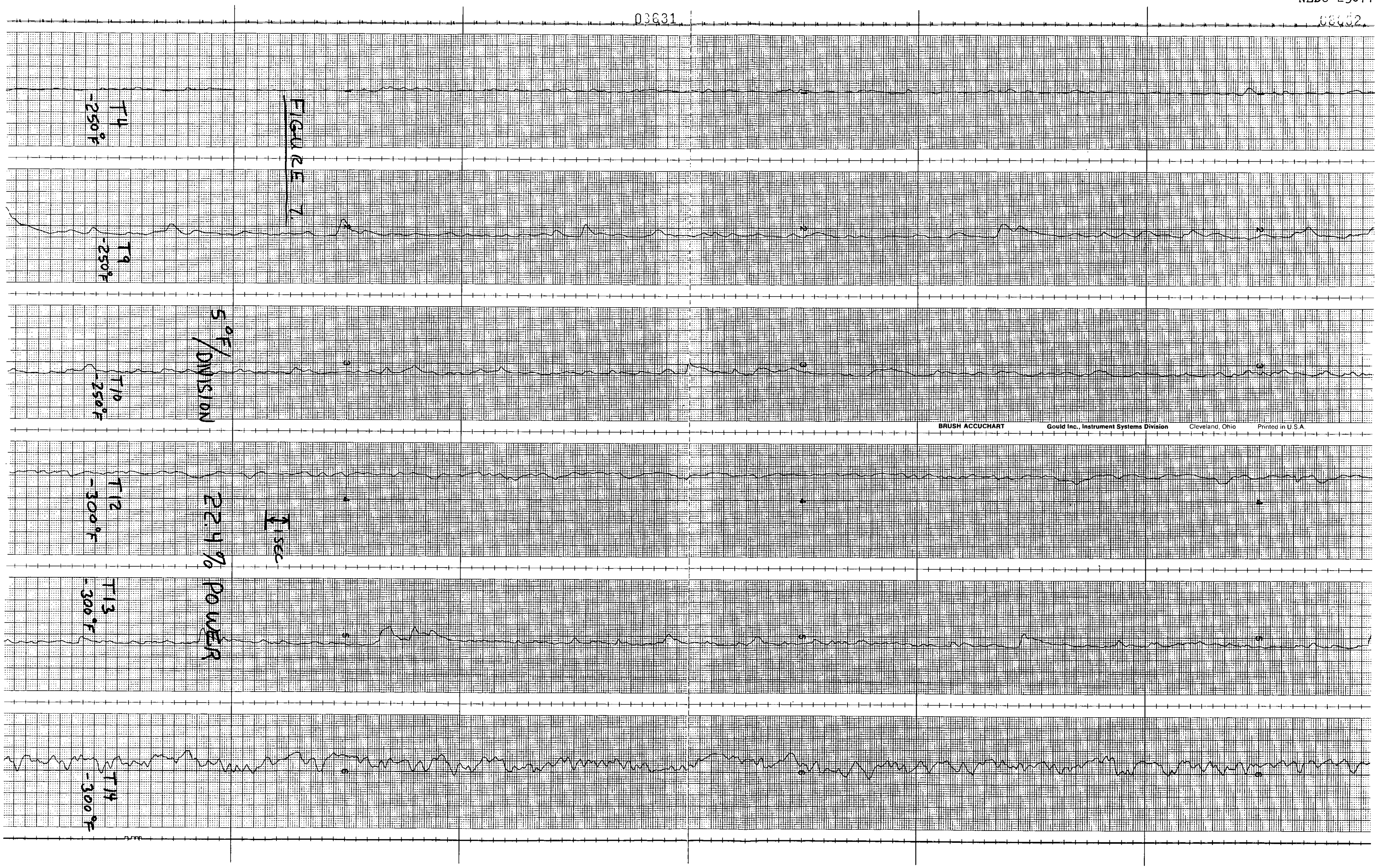

Figure 3-7. Temperature Cycling 22.4% Power Recorder 2

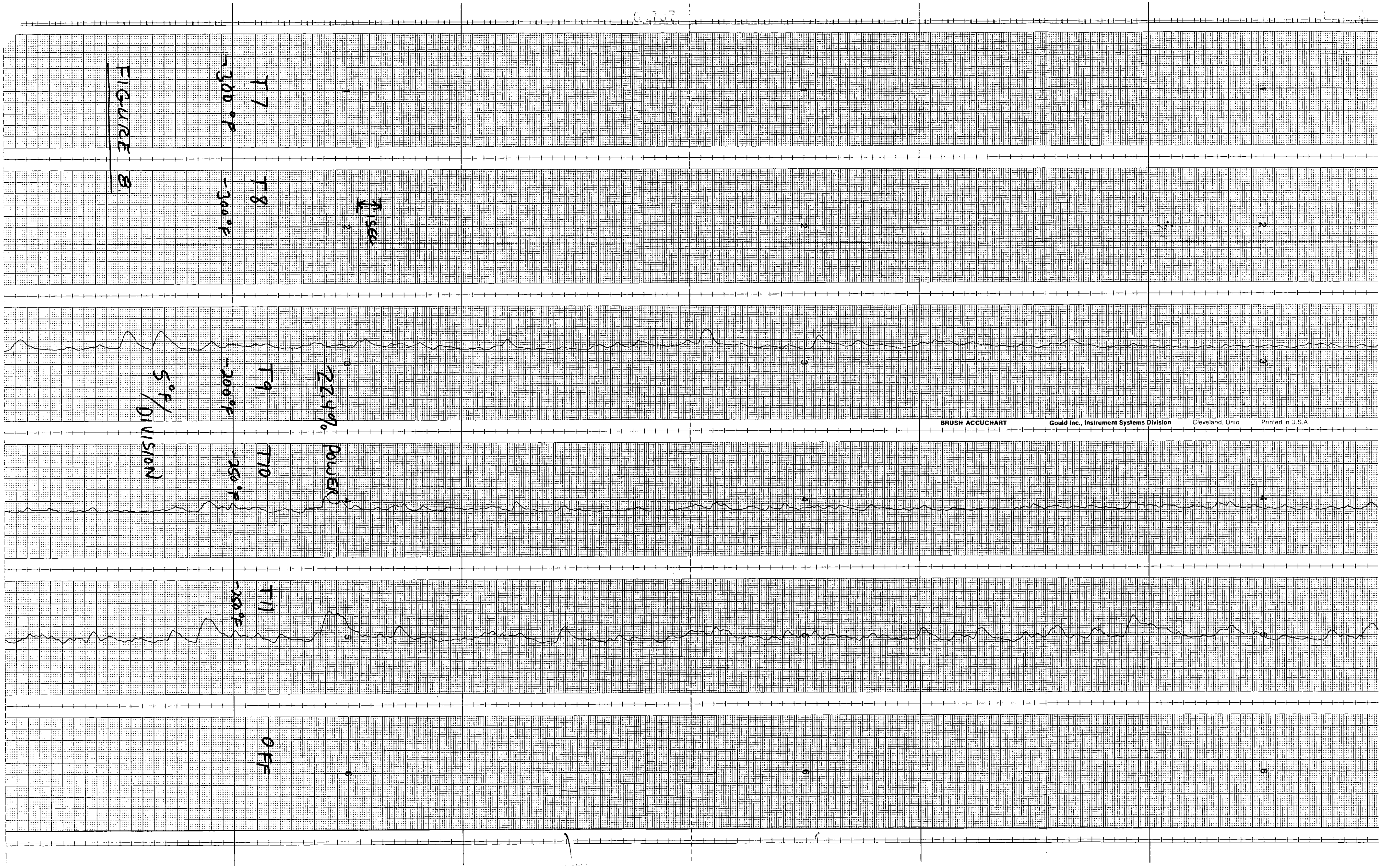

Figure 3-8. Temperature Cycling 22.4% Power Recorder 3

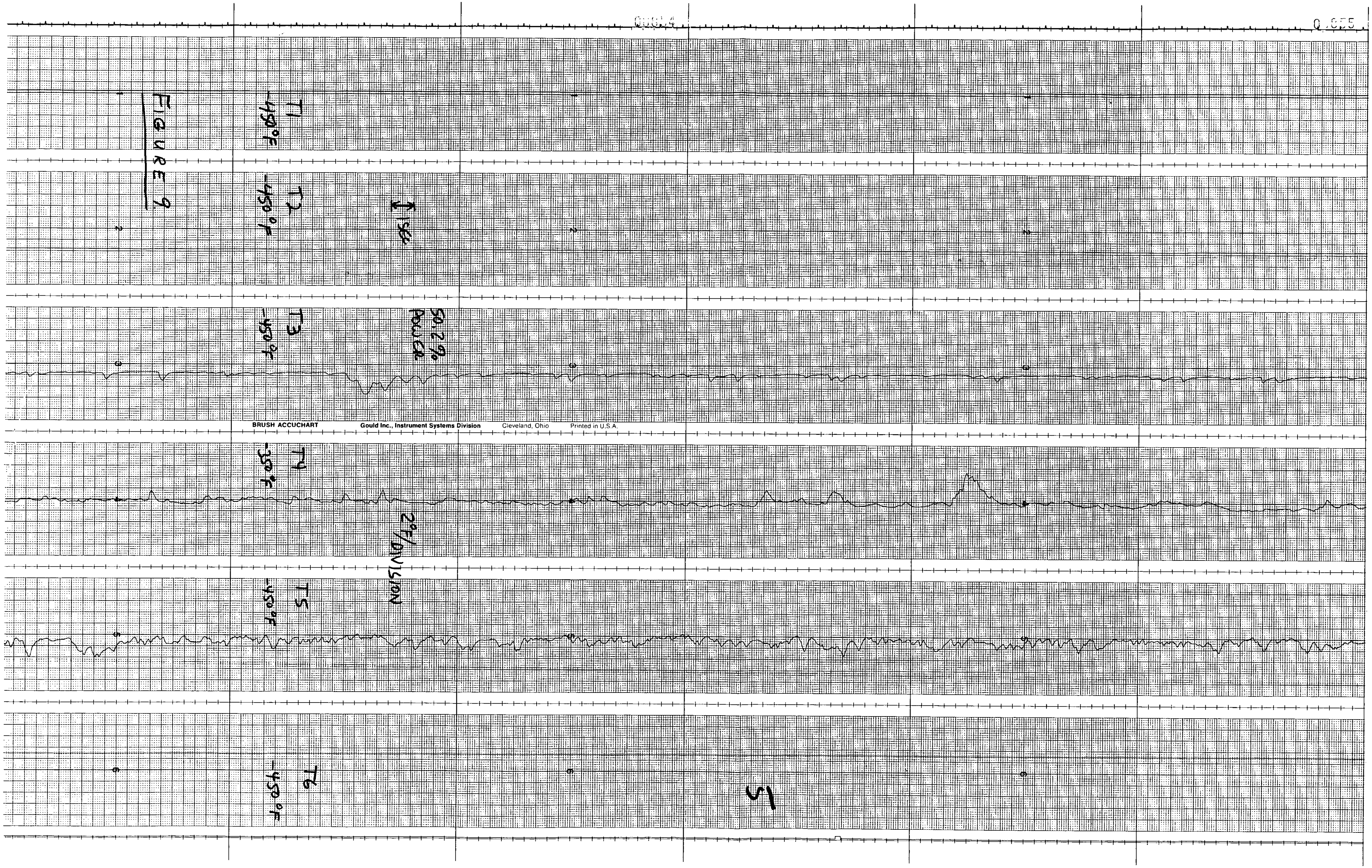

Figure 3-9. Temperature Cycling 50.2% Power Recorder 1

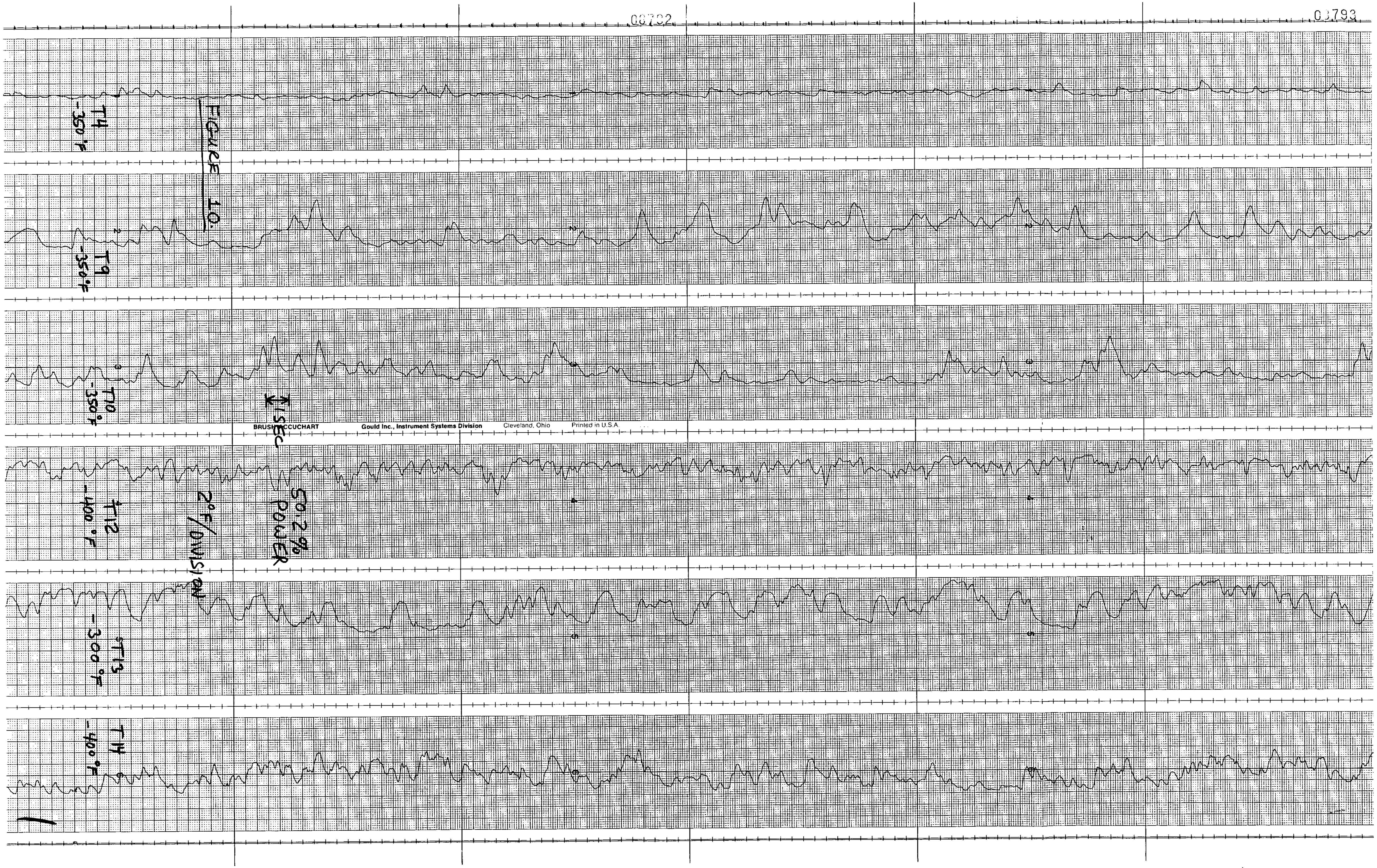

Figure 3-10. Temperature Cycling 50.2% Power Recorder 2

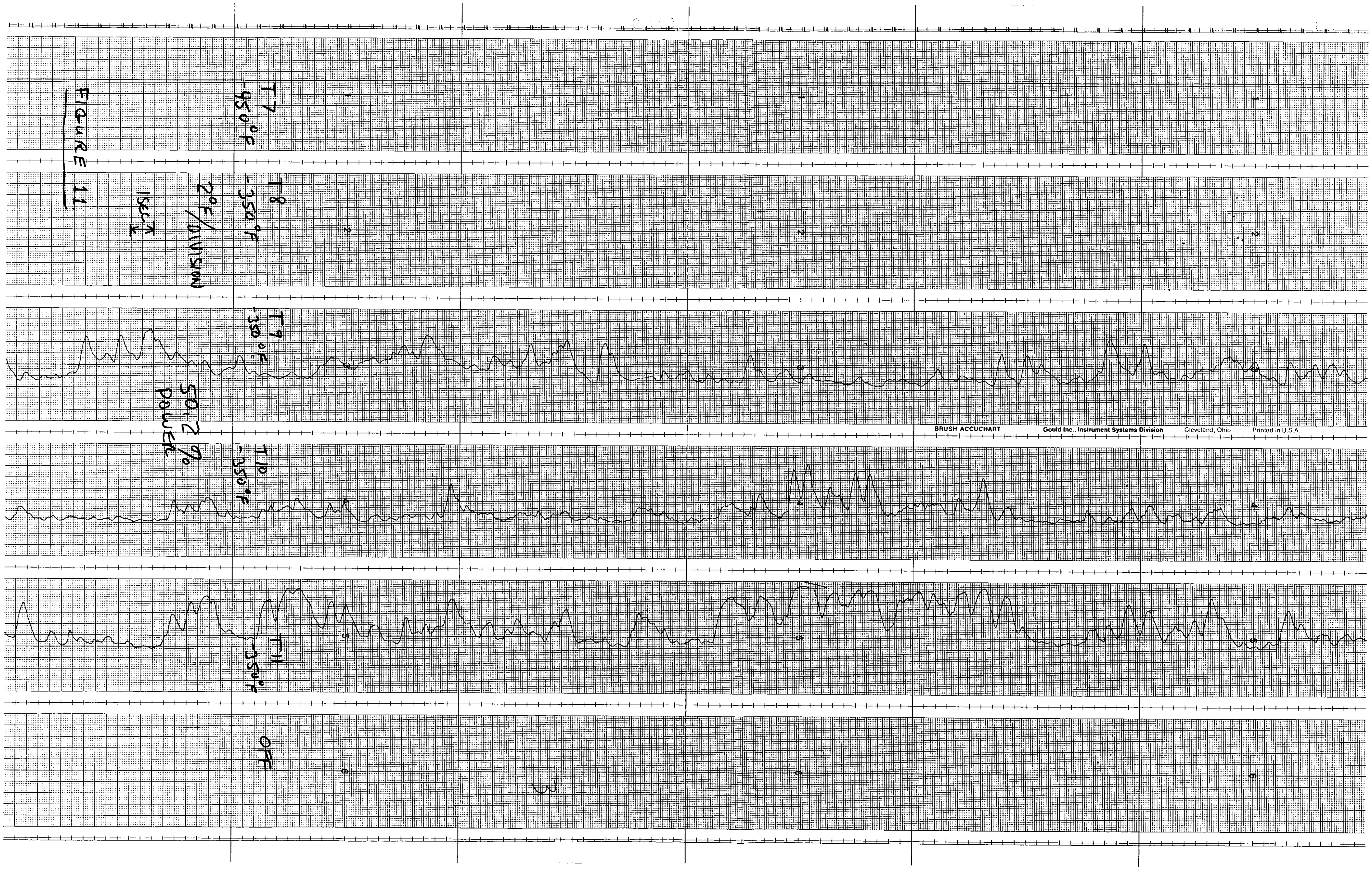

Figure 3-11. Temperature Cycling 50.2% Power Recorder 3

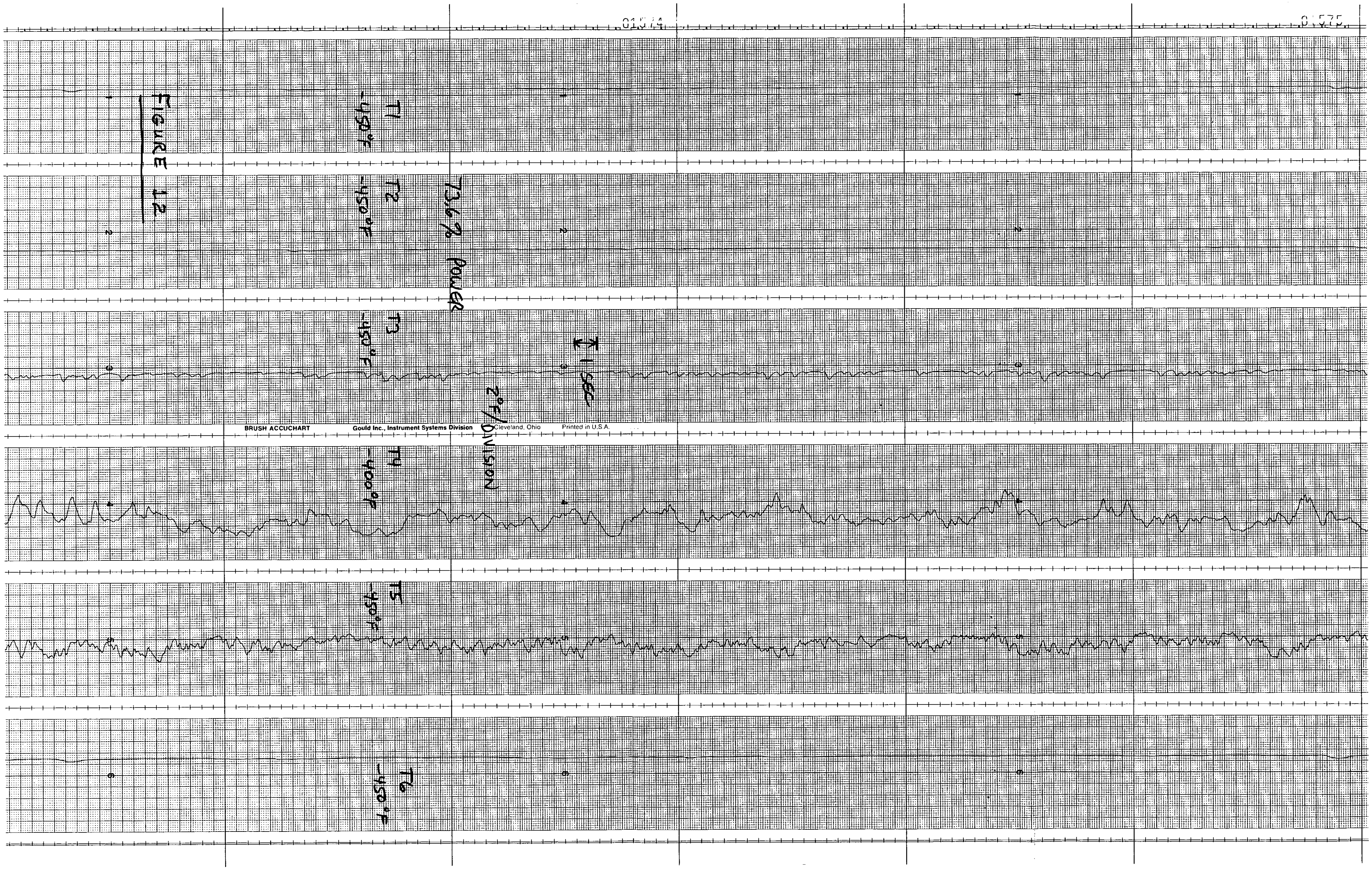

Figure 3-12. Temperature Cycling 73.6% Power Recorder 1

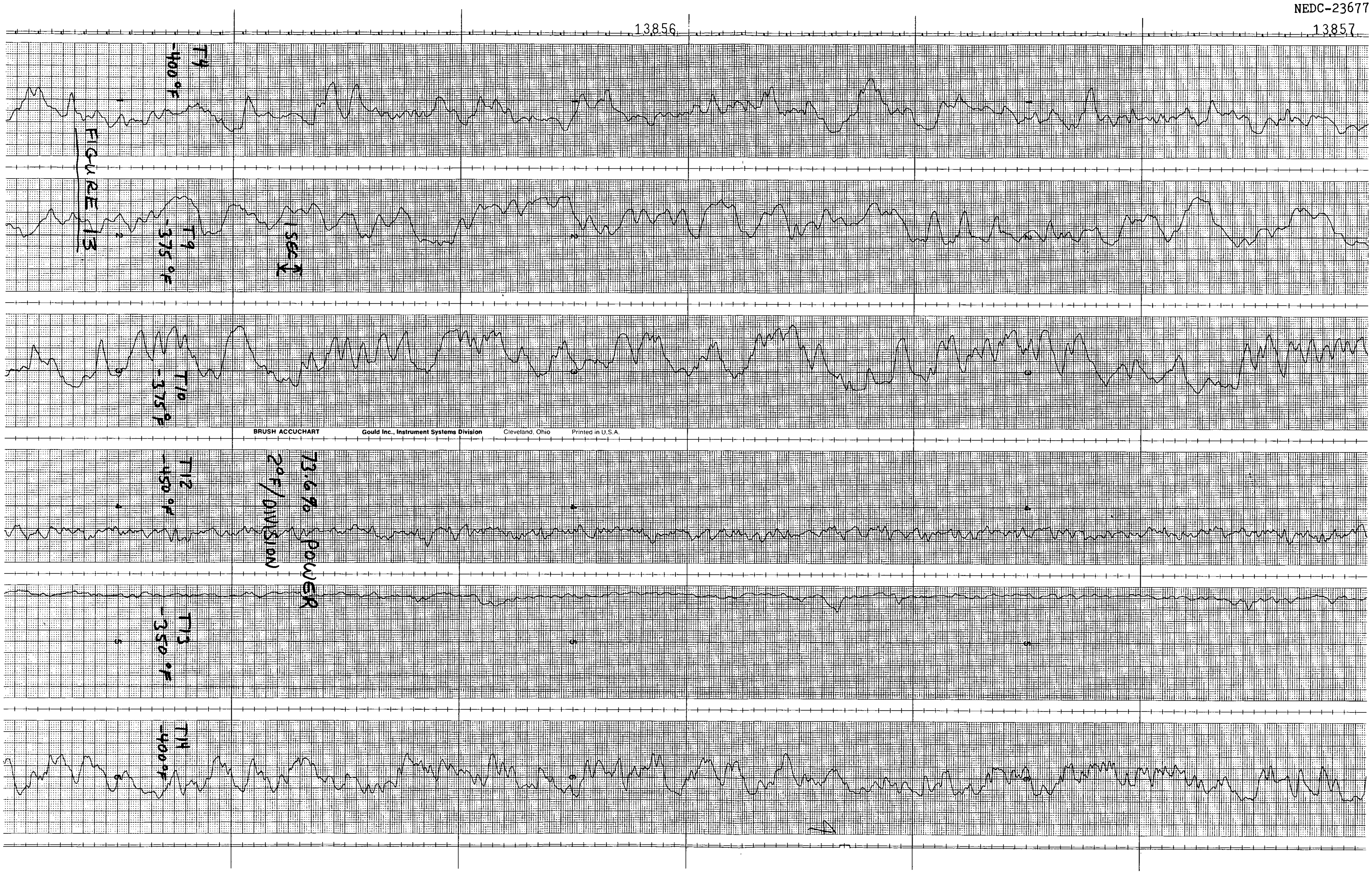

Figure 3-13. Temperature Cycling 73.6% Power Recorder 2

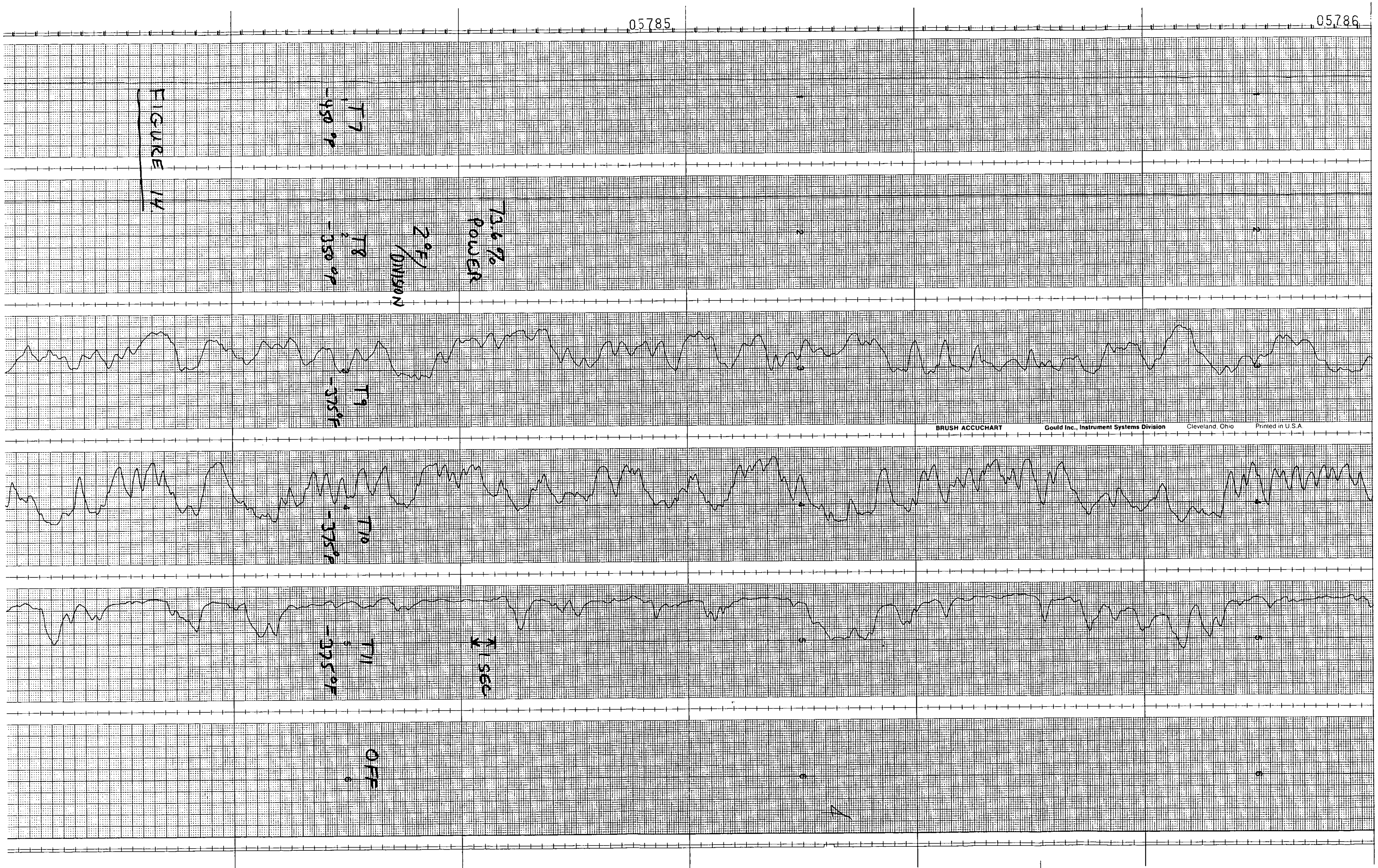

Figure 3-14. Temperature Cycling 73.6% Power Recorder 3

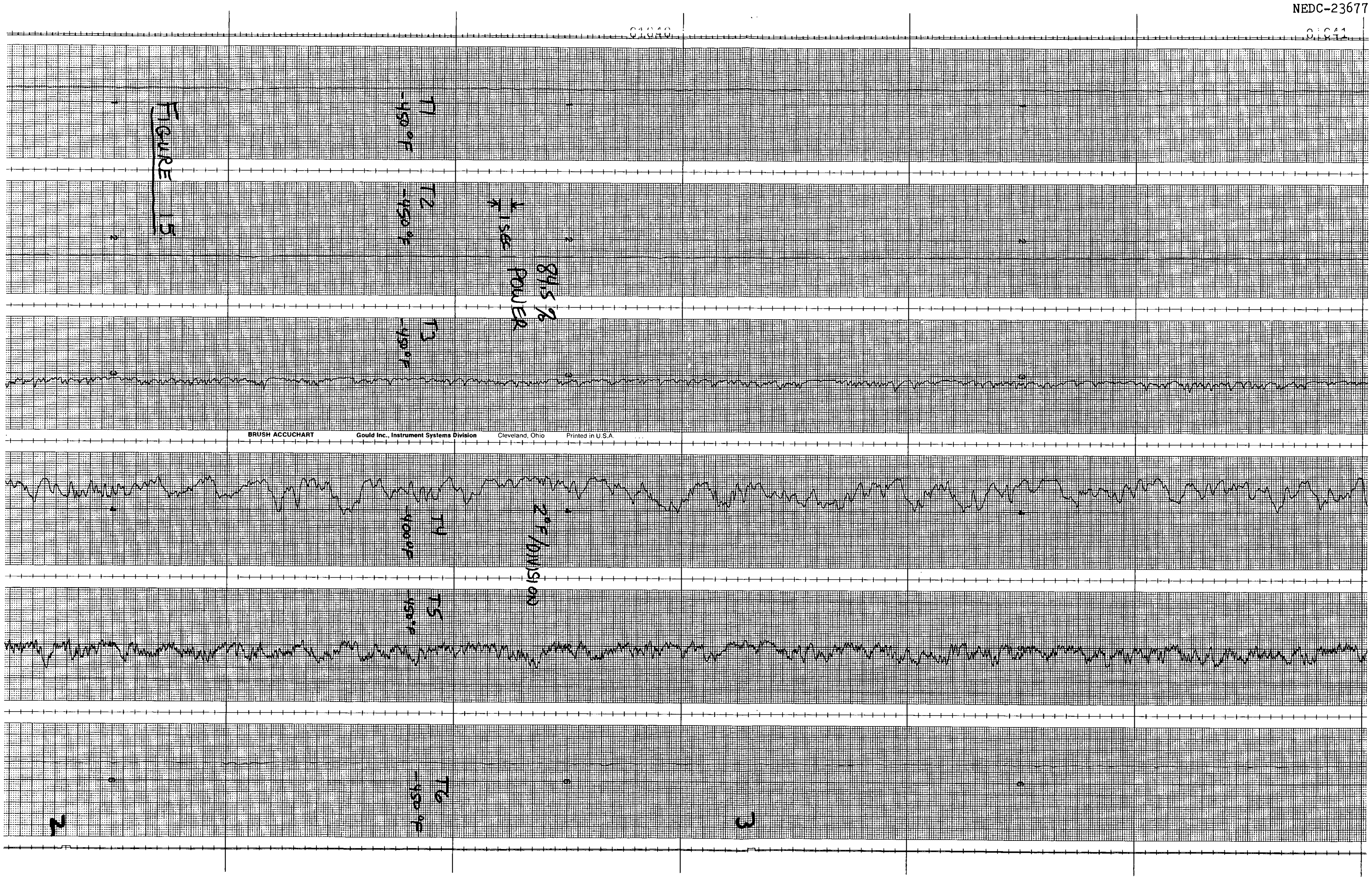

Figure 3-15. Temperature Cycling 84.5% Power Recorder 1

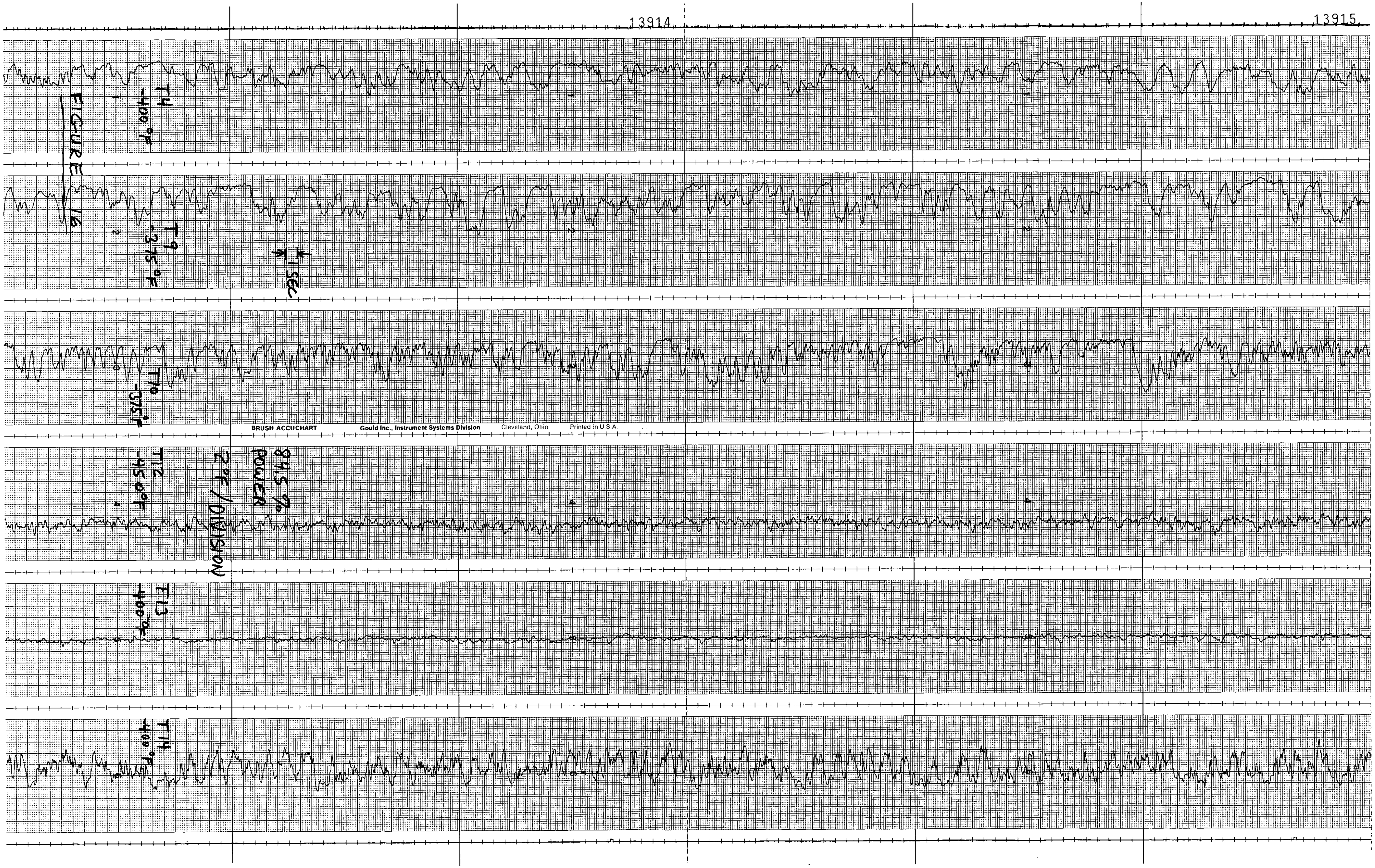

Figure 3-16. Temperature Cycling 84.5% Power Recorder 2

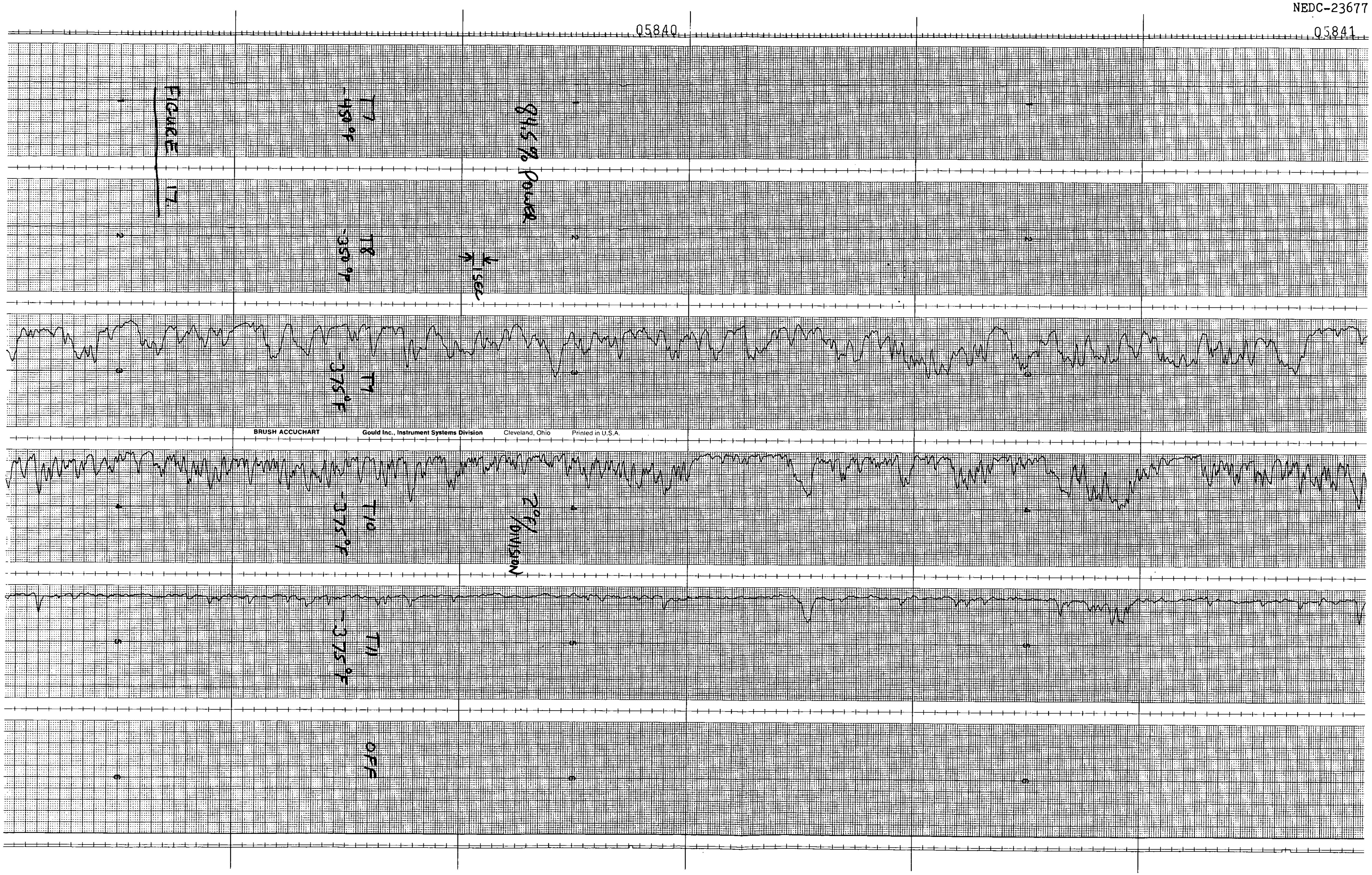

Figure 3-17. Temperature Cycling 84.5% Power Recorder 3

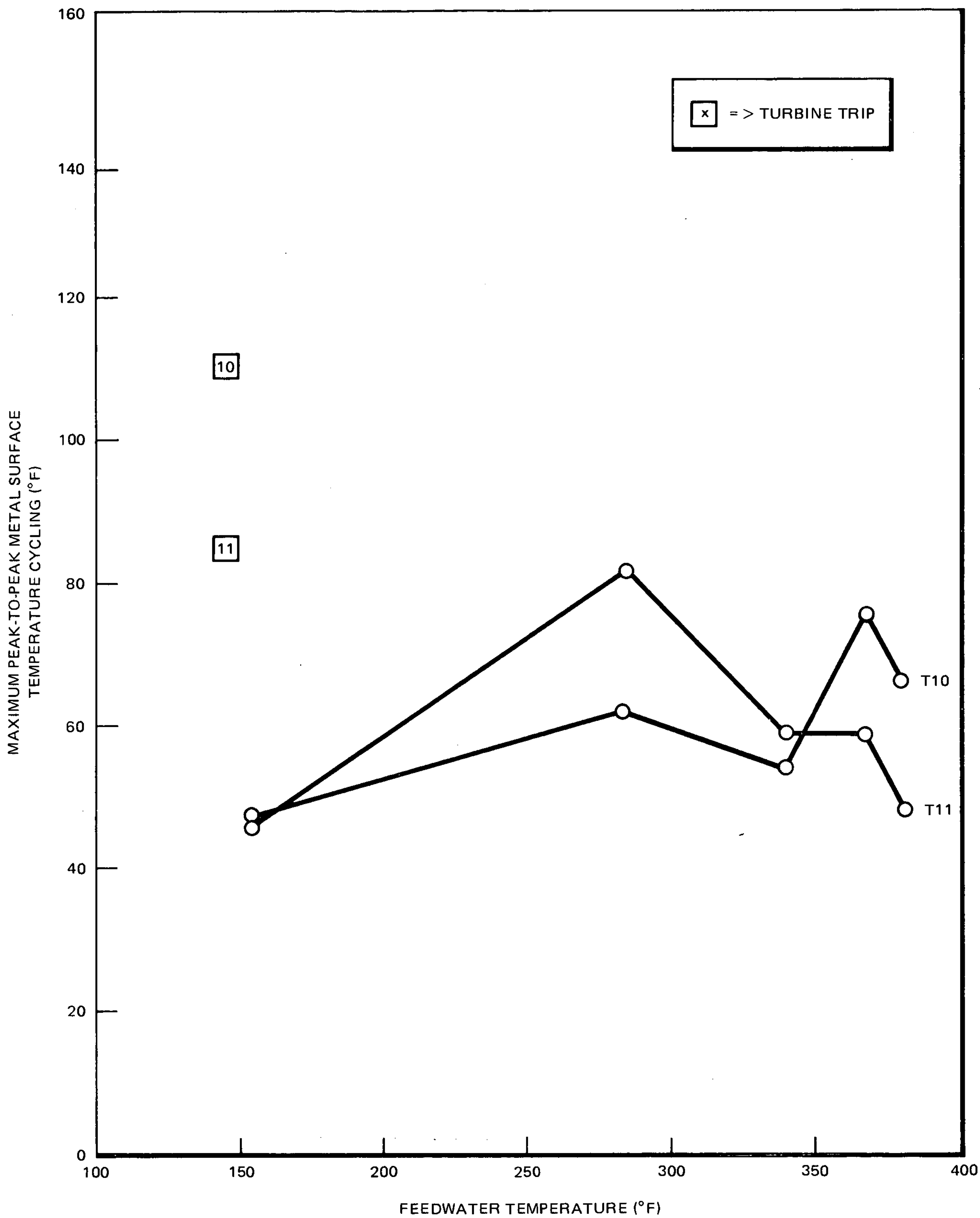

Figure 3-18. Temperature Cycling N4A(45°) Nozzle

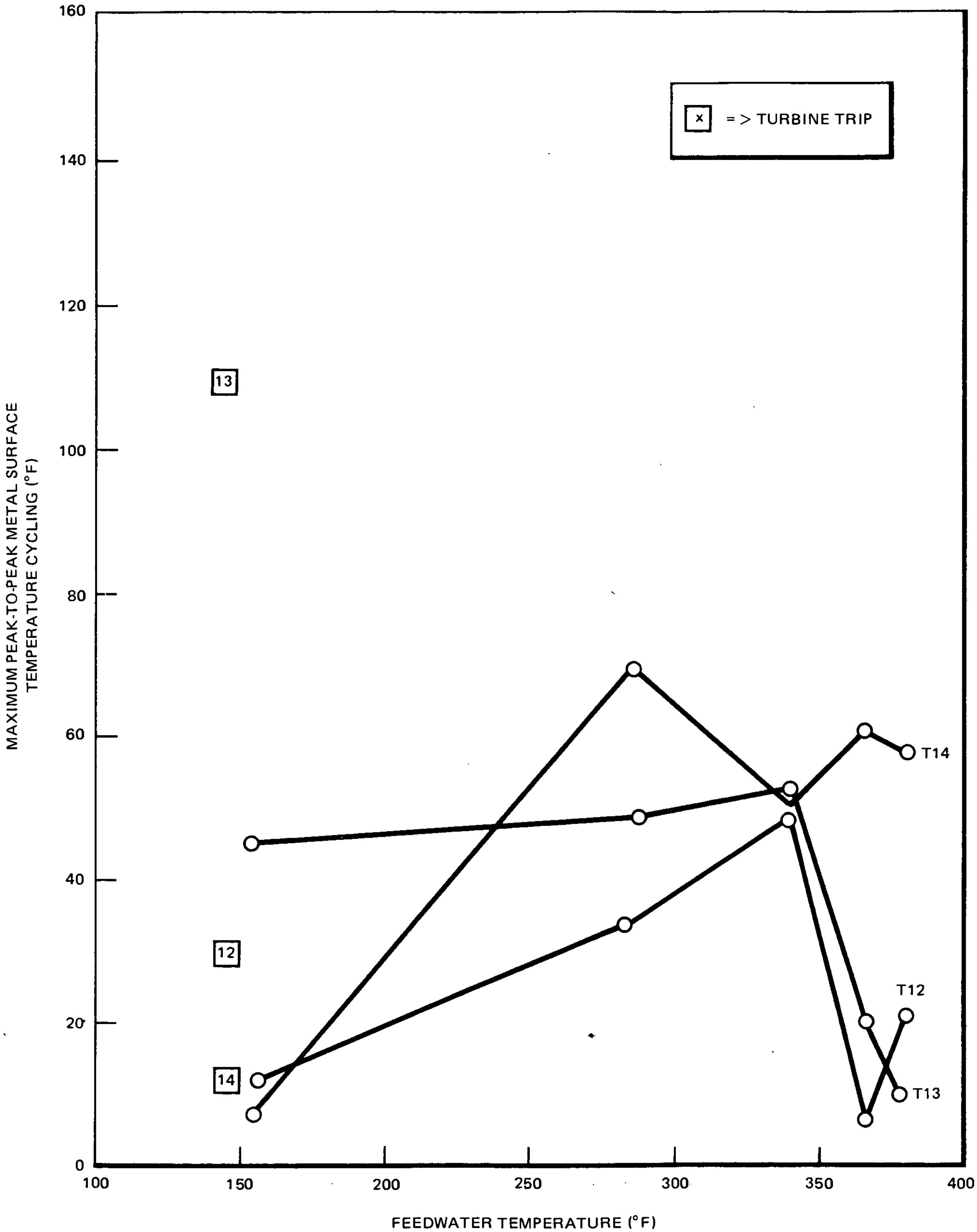

Figure 3-19. Temperature Cycling N4B (135°) Nozzle

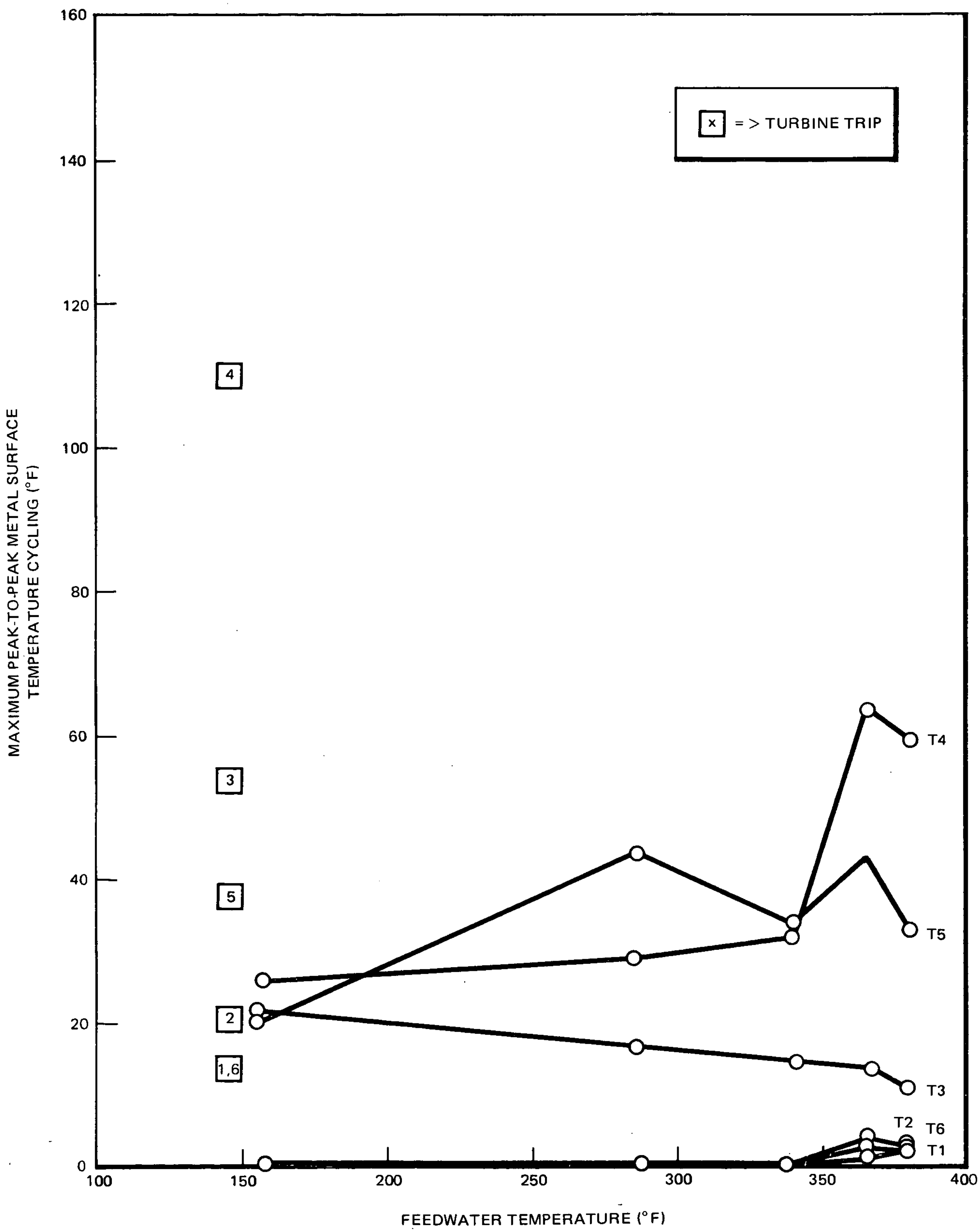

Figure 3-20. Temperature Cycling N4C (225°) Nozzle

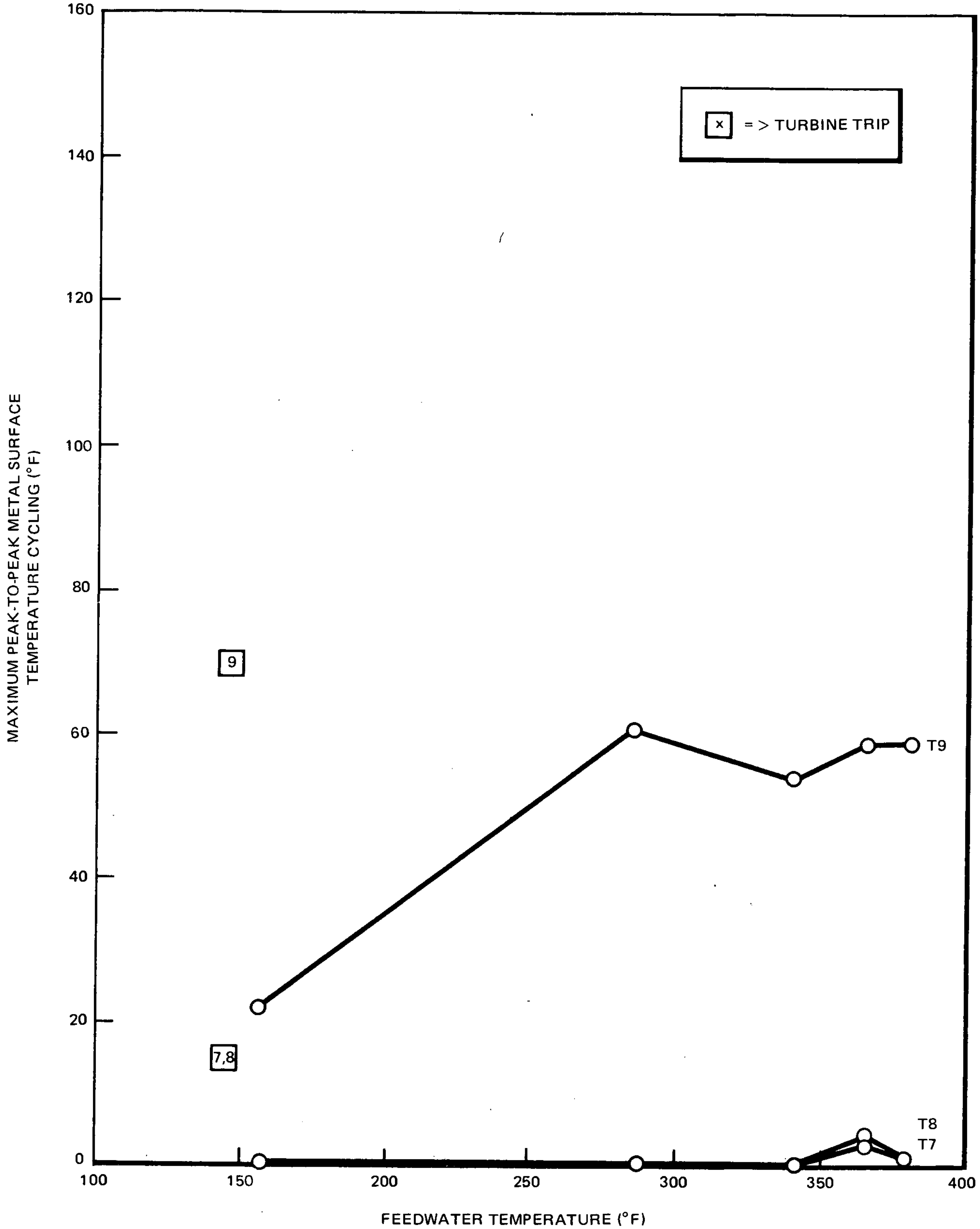

Figure 3-21. Temperature Cycling N4D (315°) Nozzle

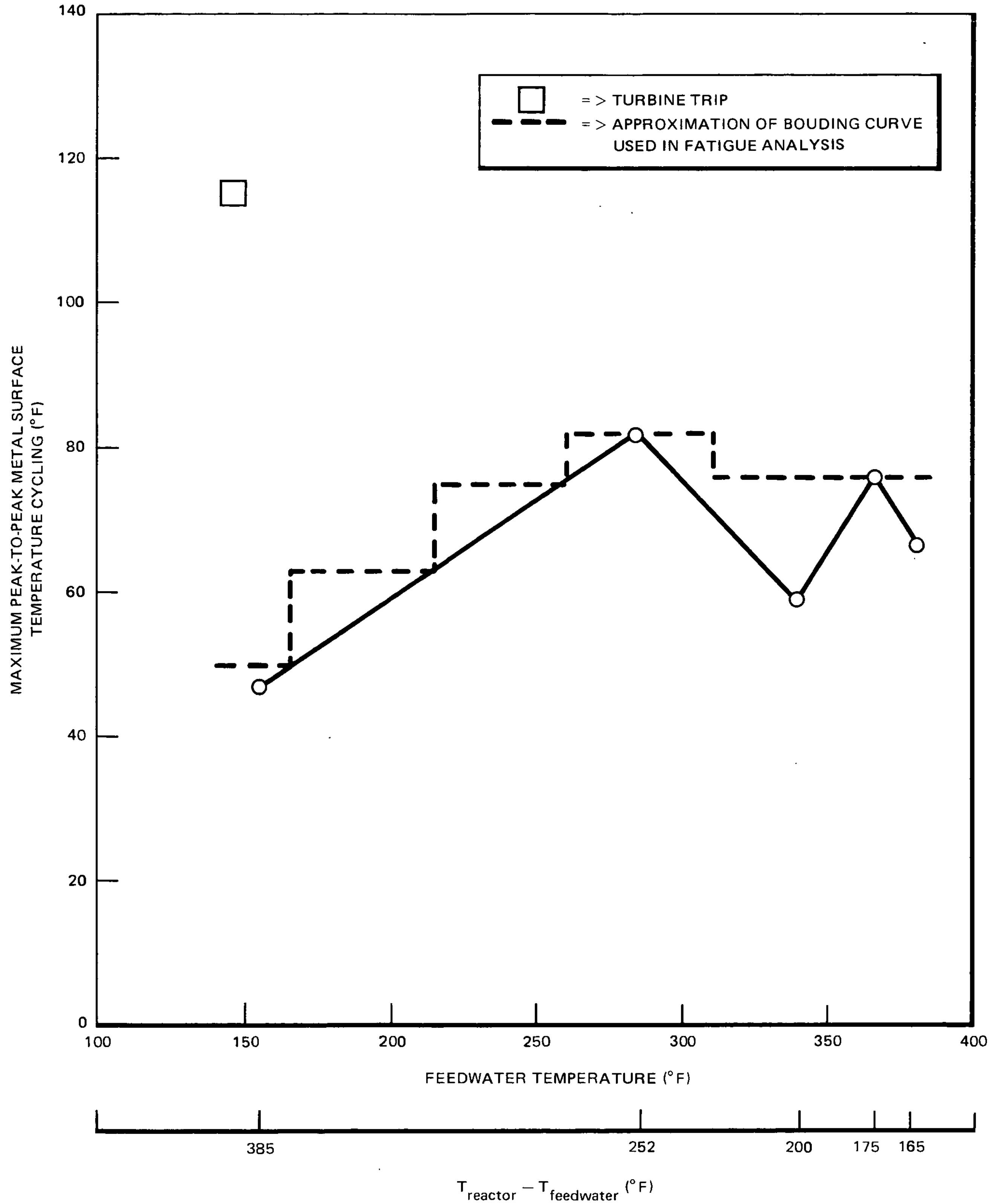

Figure 3-22. Temperature Cycling Bounding Curve

Table 3-1

MAXIMUM PEAK-TO-PEAK TEMPERATURE RANGE (ΔT) IN APPROXIMATELY 4-MINUTE INTERVAL

Recorder Number	RTD Number	Prior to Turbine Roll 1200 Hours 5/13/77			Turbine Trip 1830 Hours 5/13/77			22.4% Power 0330 Hours 5/14/77			50.2% Power 1500 Hours 5/15/77			73.6% Power 0930 Hours 5/19/77			84.5% Power 1350 Hours 5/20/77		
		$T_{feedwater}$	$T_{reactor}$	ΔT	$T_{feedwater}$	$T_{reactor}$	ΔT	$T_{feedwater}$	$T_{reactor}$	ΔT	$T_{feedwater}$	$T_{reactor}$	ΔT	$T_{feedwater}$	$T_{reactor}$	ΔT	$T_{feedwater}$	$T_{reactor}$	ΔT
	1	154°F	539°F	0°F	149°F	NA*	15°F	285°F	537°F	0°F	340°F	540°F	0°F	367°F	542°F	3°F	378°F	543°F	2°F
	2	154°F	539°F	0	149°F	NA*	20	285°F	537°F	0	340°F	540°F	1	367°F	542°F	3	378°F	543°F	3
	3	154°F	539°F	15	149°F	NA*	54	285°F	537°F	22	340°F	540°F	15	367°F	542°F	14	378°F	543°F	11
1	4	154°F	539°F	26	149°F	NA*	110	285°F	537°F	29	340°F	540°F	32	367°F	542°F	64	378°F	543°F	60
	5	154°F	539°F	20	149°F	NA*	38	285°F	537°F	44	340°F	540°F	34	367°F	542°F	43	378°F	543°F	33
	6	154°F	539°F	0	140°F	NA*	20	285°F	537°F	0	340°F	540°F	0	367°F	542°F	4	378°F	543°F	3
	4	154°F	539°F	5	149°F	NA*	115	285°F	537°F	31	340°F	540°F	32	367°F	542°F	62	378°F	543°F	59
	9	154°F	539°F	25	149°F	NA*	75	285°F	537°F	62	340°F	540°F	52	367°F	542°F	59	378°F	543°F	60
	10	154°F	539°F	40	149°F	NA*	112	285°F	537°F	62	340°F	540°F	54	367°F	542°F	76	378°F	543°F	67
2	12	154°F	539°F	12	149°F	NA*	30	285°F	537°F	34	340°F	540°F	49	367°F	542°F	7	378°F	543°F	22
	13	154°F	539°F	45	149°F	NA*	113	285°F	537°F	49	340°F	540°F	53	367°F	542°F	21	378°F	543°F	10
	14	154°F	539°F	8	149°F	NA*	12	285°F	537°F	70	340°F	540°F	51	367°F	542°F	61	378°F	543°F	58
	7	154°F	539°F	0	149°F	NA*	15	285°F	537°F	0	340°F	540°F	0	367°F	542°F	3	378°F	543°F	1
	8	154°F	539°F	0	149°F	NA*	15	285°F	537°F	0	340°F	540°F	0	367°F	542°F	4	378°F	543°F	1
3	9	154°F	539°F	22	149°F	NA*	70	285°F	537°F	61	340°F	540°F	54	367°F	542°F	59	378°F	543°F	59
	10	154°F	539°F	47	149°F	NA*	110	285°F	537°F	64	340°F	540°F	55	367°F	542°F	72	378°F	543°F	67
	11	154°F	539°F	46	149°F	NA*	85	285°F	537°F	82	340°F	540°F	59	367°F	542°F	59	378°F	543°F	48
	SNA	154°F	539°F	-	149°F	NA*	-	285°F	537°F	-	340°F	540°F	-	367°F	542°F	-	378°F	543°F	47
Spares	SNB	154°F	539°F	-	149°F	NA*	-	285°F	537°F	-	340°F	540°F	-	367°F	542°F	-	378°F	543°F	22
	SNC	154°F	539°F	-	149°F	NA*	-	285°F	537°F	-	340°F	540°F	-	367°F	542°F	-	378°F	543°F	48
	SND	154°F	539°F	-	149°F	NA*	-	285°F	537°F	-	340°F	540°F	-	367°F	542°F	-	378°F	543°F	49

RTD readings have been corrected to the actual temperature with the calibration curve.

*The pressure sensors recorded a reactor pressure of 0.0 psig. Thus the reactor temperature is unknown.

raw data (Figure 3-8) will show that the 82°F cycling was infrequent. Most cycles had peak-to-peak amplitudes substantially less than 82°F.

RTD SNA shows that the maximum cycling is restricted to a local region as well as to one power level.

d. Generally, maximum cycling occurs at X = 0.5 and decreases as X increases.

e. Cycling is reduced as the feedwater temperature is reduced below 285°F (22.4% power).

f. Generally maximum cycling occurs at 22.4% power.

3.4.2 Time at Temperature

3.4.2.1 Iowa Electric Input

The basic data needed to generate a time temperature map for the feedwater system were supplied by Iowa Electric specifically for the Duane Arnold plant. It is tabulated below:

a. Feedwater heaters are on line 100% of the time reactor is operating.

b. There will be 3221 days of outage during the 40-year design life.

c. The startup that was monitored is typical of the 280 slow startups.

d. In addition, there will be 400 fast startups that are similar to a slow startup, except they take one-half as long.

e. Each shutdown is similar to a startup, except it takes one-tenth as long.

f. There will be 2 years of operation at 50% power and 2 years at 75% power.

g. Remainder of the 40-year design life will be spent at a power greater than 75%.

3.4.2.2 Time/Temperature Map

Table 3-2 contains the time/temperature information for the May 1977 startup. The values in Table 3-2 should be multiplied by

$$280 + \frac{400}{2} + \frac{280 + 400}{10} = 548$$

to obtain the map for all startups and shutdowns in the 40-year design life. The total number of hours of operation at greater than 75% power can be obtained in the following manner.

$$H(>75) = 30(548) + 24 \left[40(365) - (2+2)\ 365 - 3221 - \frac{548(167)}{24}\right]$$

$$= 163{,}000 \text{ hours}$$

$H(>75)$ = Hours of Operation at Greater than 75% Power

The number of hours at 50% power plus the number of hours at 75% power can be calculated in the following manner:

$$H(50\% \text{ to } 75\%) = (2+2)\ 365\ (24) + 96\ (548) = 87{,}600 \text{ hours}$$

Thus, the 40-year design life map is tabulated in Table 3-3.

3.5 CRITERIA

Feedwater nozzle cracks are initiated by cyclic stress. The fatigue usage factor at the blend radius due to stress cycles considered in the reactor pressure vessel stress report[9] is approximately 0.6. The ASME Section III allowable value is 1.0.

Table 3-2
MAY 1977 STARTUP MAP

$T_{reactor} - T_{feedwater}$	Hours of Operation
$500^{o}F \pm 25^{o}F$	0
$450^{o}F \pm 25^{o}F$	0
Turbine Trip	1
$400^{o}F \pm 25^{o}F$	7
$350^{o}F \pm 25^{o}F$	4
$300^{o}F \pm 25^{o}F$	8
$250^{o}F \pm 25^{o}F$ (≈25% power)	21
$200^{o}F \pm 25^{o}F$ (50 to 75% power)	96
$150^{o}F \pm 25^{o}F$ (>75% power)	30
TOTAL HOURS	167

NOTE

$T_{reactor}$ = Saturation temperature at reactor pressure

$T_{feedwater}$ = The average temperature of the two feedwater lines

Table 3-3

40-YEAR DESIGN LIFE TIME/TEMPERATURE MAP

$T_{reactor} - T_{feedwater}$		Hours of Operation
$500^{\circ}F \pm 25^{\circ}F$		0
$450^{\circ}F \pm 25^{\circ}F$		0
Turbine Trip		550
$400^{\circ}F \pm 25^{\circ}F$		3,800
$350^{\circ}F \pm 25^{\circ}F$		2,200
$300^{\circ}F \pm 25^{\circ}F$		4,400
$250^{\circ}F \pm 25^{\circ}F$		11,500
$200^{\circ}F \pm 25^{\circ}F$		87,600
$150^{\circ}F \pm 25^{\circ}F$		163,000
0		77,300
	TOTAL	350,350

Fatigue usage on the blend radius was not explicitly calculated in Reference 9. Fatigue usage was calculated for the nozzle and safe end region. The safe end and the weld of the thermal sleeve to the safe end were investigated in detail as it was known that the fatigue usage would be greater there than at the blend radius. The maximum calculated fatigue usage factor was 0.9 and occurred on the outside surface of the safe end. Based on a survey of latter stress reports, the fatigue usage factor on the blend radius is approximately 0.6.

Fatigue usage due to rapid thermal cycling was not explicitly included in the Duane Arnold design. Thus, a usage factor allowance of up to 0.4 remains for rapid thermal cycling.

If the fatigue usage factor due to rapid thermal cycling can be shown to be less than 0.4 during the reactor design life, then the feedwater nozzle would not be expected to experience fatigue cracking. If the fatigue usage factor was shown to be greater than 0.13 per year (5.0 in 40 years), then cracks would be expected to have occurred before the next refueling outage. If the fatigue usage factor is greater than 0.4 and less than 5.0, then the analysis is not conclusive.

3.6 ANALYSIS

Fatigue damage due to rapid thermal cycling is evaluated utilizing the Ordered Overall Range (OOR) cycle counting approach of References 10 and 11, in conjunction with the General Electric extrapolation of the ASME Boiler and Pressure Vessel Code Section III fatigue curve for stainless steel.

3.6.1 Cycle Counting Technique

The subject of fatigue under random loading cycling has been extensively researched in connection with automotive, aerospace and highway bridge applications. Several methods for estimating fatigue damage under random cycling are available in the literature. Some of the methods make use of the statistical character of the cycle pattern, as characterized by mean and standard deviation of the signal. Others involve a brute force cycle counting approach in which the fatigue damage contribution of each individual cycle is calculated and summed to estimate total fatigue damage. Because the thermal cycling from General Electric tests does not adhere to any consistent statistical distribution (such as normal or Gaussian), it was found that statistical approaches could not be conveniently applied, and it was necessary to resort to a cycle counting approach to evaluate fatigue damage. The OOR approach of References 10 and 11 was selected to perform the cycle counting.

The OOR is an abbreviated cycle counting approach, which permits selection of a small number of load reversals which account for a large fraction of the fatigue damage. Figure 3-23 illustrates application of the approach to a simplified load trace. The first step is to select the largest overall range of a load (or temperature) trace, from the highest peak to the lowest valley (points F and U in Figure 3-23). Next a screening level of some percentage of the largest overall range (50% in Figure 3-23) is selected and ranges with amplitudes greater than the screening level are counted, keeping track of the sequence in which the reversals occur. Only reversals which occur in a peak-valley-peak-valley sequence are considered in counting ranges greater than the screening level.

(Note that in Figure 3-23, the range between reversals H and M is actually larger than the counted range between M and R, but the former range was not counted because it was not in the correct sequence and would yield a peak-peak-valley-valley sequence in conjunction with the largest overall range.) The screening level is then reduced incrementally to zero, and a load spectrum of screening amplitude versus number (or percent) of cycles greater than the screening amplitude is produced as illustrated at the bottom of Figure 3-23. The finer the screening level increments, the more accurate will be the representation of the actual cycling.

The resulting OOR load spectrum can be used to estimate fatigue damage in conjunction with any fatigue curve and cumulative damage law desired. In many cases, only the upper portion of the load spectrum is required to obtain a reasonably accurate damage estimate since higher stress cycles tend to dominate fatigue damage calculations.

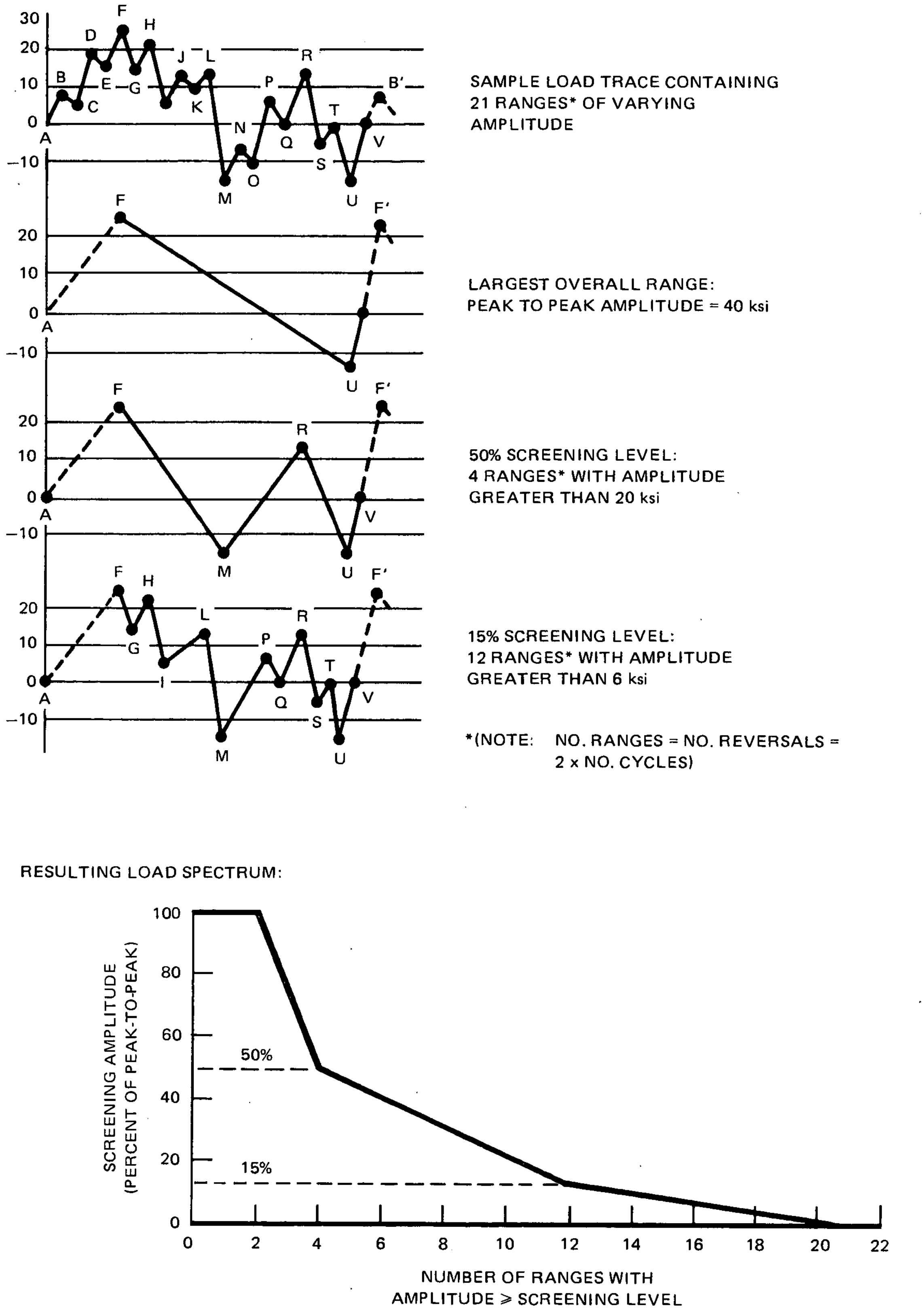

Figure 3-23. Illustration of Ordered Overall Range (OOR) Cycle Counting Approach

3.6.2 Envelope Load Spectrum

Based on General Electric tests, an envelope load spectrum has been developed (Figure 3-24). This envelope spectrum should be applicable, with a reasonable degree of conservatism, to any temperature trace of the test program. Two of the highest Duane Arnold cyclic locations have been compared to the envelope load spectrum. The results are also shown on Figure 3-24. The high power case falls on the envelope curve and the low power case falls substantially below the envelope curve. Thus, fatigue damage predictions based on the envelope curve will be accurate for high power operation and conservative for low power operation. Inspection of the typical temperature traces (Figures 3-6 through 3-17) will reinforce this conclusion. During high power operation there are many temperature cycles that approach the maximum peak-to-peak cycle; while during low power operation, most temperature cycles are small compared to the maximum peak-to-peak cycle.

3.6.3 Fatigue Evaluation Method

The envelope load spectrum of Figure 3-24 has been changed into a table containing the number of cycles at various amplitudes (A) as shown in Table 3-4. Since the test traces analyzed were approximately 240 seconds long, the envelope spectra of Figure 3-24 results in discreet numbers of cycles at each amplitude per 240 seconds of cycling, and must be scaled up or down to the actual cycling duration. In the last column of Table 3-4 the cycling has been scaled up to indicate the number of cycles at various amplitudes per hour of cycling. Note that a factor of two has been applied in transferring the envelope spectrum from Figure 3-24 to Table 3-4 to translate from reversals to cycles (two reversals/cycle).

The last column of Table 3-4 can now be used to compute fatigue damage per hour of cycling at any peak stress level by summing the damage from 15 cycles of amplitude equal to 98% of the peak stress level, 30 cycles of amplitude equal to 93% of the peak stress level, etc.

For consistency with ASME code design procedures and General Electric design requirements, the design fatigue curves of Figure 3-25 were used in performing the damage calculations. The austenitic stainless steel fatigue curve of Figure

Table 3-4
ENVELOPE SPECTRUM FOR FATIGUE DAMAGE CALCULATON

Screening Amplitude A (%)	Total Number of Cycles A	$\bar{A}$%	Number* of Cycles (240 sec)	Number* of Cycles (hr)
100	0			
		98	1	15
96	1			
		93	2	30
90	3			
		88	2	30
86	5			
		83	5	75
80	10			
		75	8	120
70	18			
		65	10	150
60	8			
		55	12	180
50	40			
		45	15	225
40	55			
		35	25	375
30	80			
		25	25	375
20	105			
		15	75	1125
10	180			

*At Amplitude = $\bar{A}$

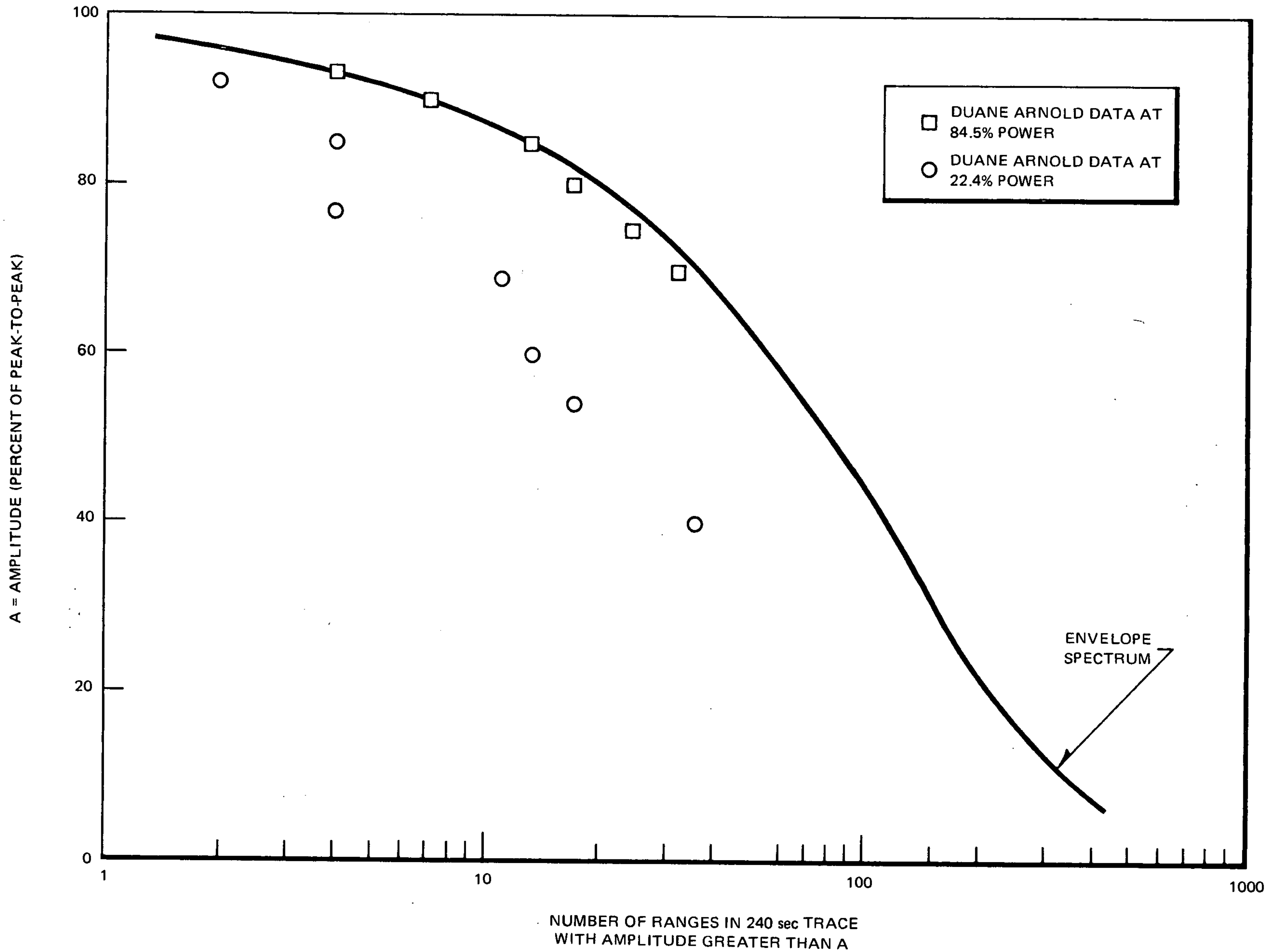

Figure 3-24. Load Spectra

3-25 was used as the Duane Arnold feedwater nozzles are clad. Peak stress amplitudes were calculated as follows.

$$S_a = \sigma_{alternating} = \frac{E\alpha}{2(1-\mu)} \Delta T_{p-p(\%)} (T_{reactor} - T_{feedwater})$$

Where: $\frac{E\alpha}{(1-\mu)}$ = 375 psi/°F for stainless steel cladding

$\Delta T_{p-p(\%)}$ = Peak-to-peak ΔT (in percent of available temperature differential)

$T_{reactor} - T_{feedwater}$ = Available temperature differential (°F)

Figure 3-26 is a plot of fatigue damage from the above equation for several values of $\Delta T_{p-p(\%)}$.

The damage curve of Figure 3-26 represents a convenient design tool for evaluation of the thermal cycling data. The peak-to-peak cycling amplitude in percent can be obtained from the test data and, in conjunction with the load map of time versus feedwater to reactor temperature differential, can be used to enter the appropriate damage curve and predict cumulative fatigue usage.

3.6.4 Fatigue Evaluations

The fatigue damage due to the bounding temperature cycling curve (Figure 3-22) and the 40-year design life time temperature map (Table 3-3) can now be calculated using Figure 3-26. The calculation is summarized in Table 3-5. The highest cycling value and associated percent cycling for each ± 25°F interval was assumed constant for the entire interval (Figure 3-22). The cumulative fatigue usage factor due to rapid thermal cycling in 40 years is 0.2. The total 40-year fatigue usage factor for all identified cycles is 0.2 plus 0.6 or 0.8, which is less than the ASME Code allowable value of 1.0.

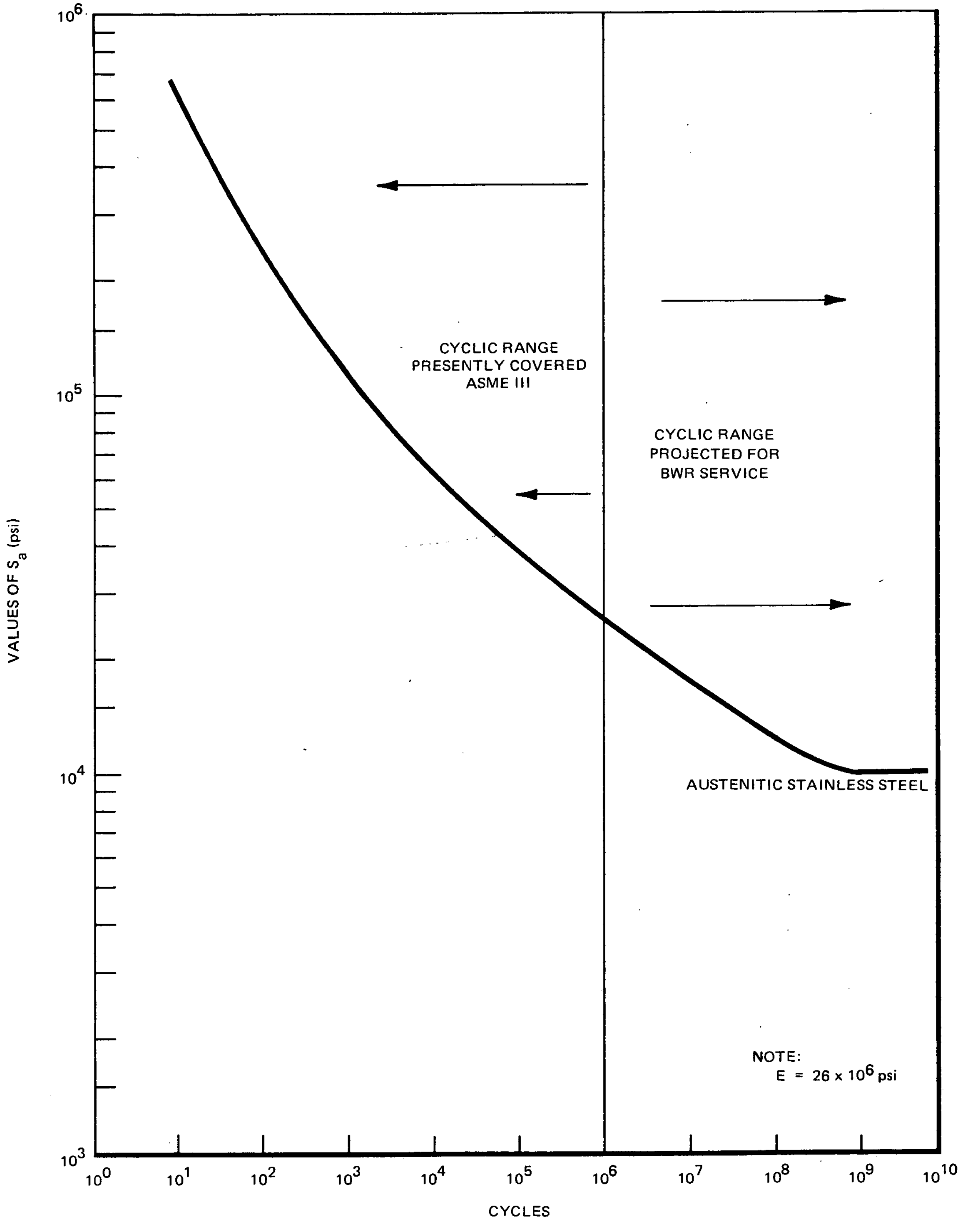

Figure 3-25. GE Extrapolation of ASME Fatigue Curve

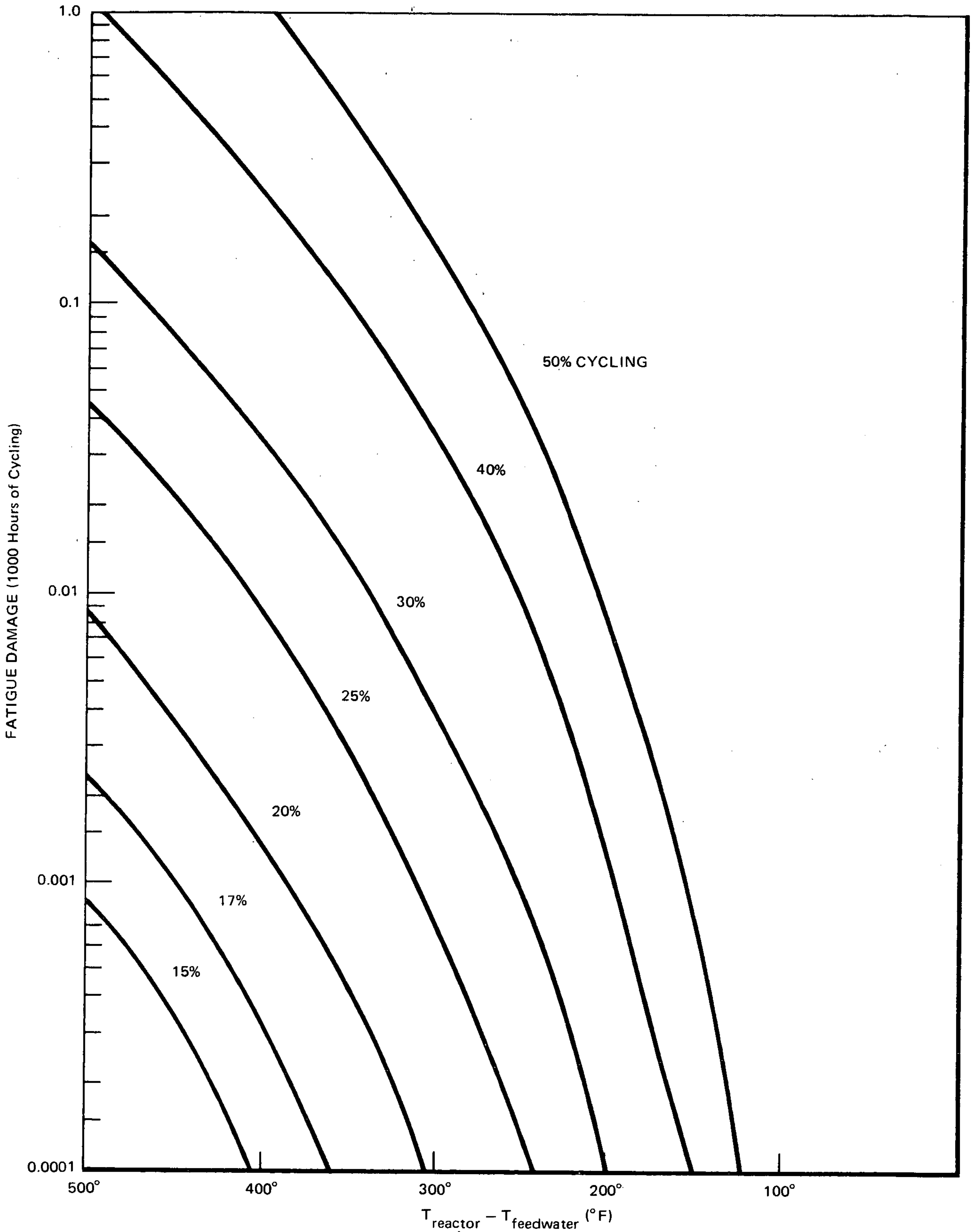

Figure 3-26. Fatigue Damage Curve

Table 3-5

CUMULATIVE FATIGUE DAMAGE

Discrete Value $T_{reactor} - T_{feedwater}$	Interval $T_{reactor} - T_{feedwater}$	Peak-to-Peak Cycling	Percent Cycling	Fatigue Damage per 1000 hr	Damage per 40-Year Life
375°F	400°F ± 25°F	50°F	13%	0.0001	0.0004
325°F	350°F ± 25°F	63°F	19%	0.00016	0.0004
275°F	300°F ± 25°F	75°F	27%	0.00065	0.0028
252°F	250°F ± 25°F	82°F	33%	0.0019	0.0219
175°F	200°F ± 25°F	76°F	43%	0.00065	0.0569
175°F	150°F ± 25°F	76°F	43%	0.00065	0.1060
	Turbine Trip*	115°F	NA	0.023	0.0127
			TOTAL		0.2011

*Percent cycling is not known for the turbine trip event. Damage during turbine trip was calculated by assuming a value of percent cycling and using Figure 3-26. This is exactly correct as figures could be directly plotted as a function of maximum peak-to-peak cycling directly without the need of obtaining the percent cycling.

The method of analysis has both conservative and nonconservative steps. The most significant of these are:

Conservatisms:

a. RTD measurements used as metal surface temperature, whereas metal surface temperature fluctuations are lower than sensor temperature fluctuations.

b. Fatigue damage curve was generated with a bounding load spectra

c. Fatigue calculation used a bounding temperature cycling curve

d. The highest temperature cycling in each $\pm 25^{o}F$ interval of the bounding curve was used for the entire interval.

Nonconservatisms:

a. A limited number (18) of RTDs were used

b. All locations of the nozzle could not be measured

c. A limited data base (one startup) was used

d. Some temperature cycles are so rapid that the RTDs may not have reached full value

The RTDs will measure a temperature that closely approximates the metal surface temperature. Tests performed by General Electric indicate that the recorded cycling is approximately 10% higher than the actual metal surface cycling.

As shown on Figure 3-24 the Duane Arnold data at high power, where most of the fatigue damage occurs, falls essentially on the bounding load spectra curve.

The bounding temperature cycling curve and the interval approximation of it were intentionally used to balance the nonconservatism due to a limited number of RTDs and the limited data base.

Based on General Electric tests, the locations of the feedwater nozzles that are expected to experience the highest temperature cycling were instrumented. It is judged that the probability of other nozzle locations having higher cycling is small.

The temperature cycling is slow enough so that the RTDs recorded at least 90% of the maximum cycling.

Therefore, it is judged that the cumulative fatigue usage factor of 0.2 is as accurate as can reasonably be calculated.

4.0 REFERENCES

1. Chicago Bridge and Iron Co. Drawing Special Forgings Nozzles N4A through N4D VPF 2655-238.

2. Chicago Bridge and Iron Co. Drawing Feedwater Nozzle VPF 2655-99.

3. Chicago Bridge and Iron Co. Drawing Thermal Sleeves for Feedwater Nozzles VPF 2655-100.

4. General Electric Co. Drawing, Reactor Assembly 197R608.

5. General Electric Co. Specification 21A2110, Feedwater Nozzle Instrumentation Program.

6. General Electric Co. Drawing 768E476, Feedwater Nozzle Instrumentation Connection Diagram.

7. General Electric Co. Drawing 768E462, Feedwater Nozzle Instrumentation Installation Kit.

8. General Electric Co. Field Deviation Disposition Requests 1001-1010, Feedwater Nozzle Instrumentation Program - DAEC.

9. DAEC Reactor Pressure Vessel Stress Report VPF 2655-330.

10. H. O. Fuchs, et al., "Shortcuts in Cumulative Damage Analysis," Society of Automotive Engineers, Paper No. 730565, 1973.

11. D. V. Nelson and H. O. Fuchs, "Predictions of Cumulative Fatigue Damage Using Condensed Load Histories," Society of Automotive Engineers, Paper No. 750045, February 1975.

DISTRIBUTION

Name	M/C
N. J. Biglieri	752
J. E. Charnley (3)	747
H. Choe	589
F. E. Cooke	747
M. Costandi (10)	873
C. W. Dillmann	752
A. B. Fife	747
J. D. Gilman	712
D. R. Heising	743
L. K. Holland	150
J. Jacobson	713
I. R. Kobsa	747
K. R. Miller	712
R. H. Moen	589
J. L. Rash	682
R. R. Roof (6)	126
H. T. Watanabe	682
NED Library (5)	328
VNC Library	V01